

ESI: A novel B,O,N-doped mesogen with narrowband MR-TADF emission

Julius A. Knöllner,^{*a} Burcu Sönmez,^a Tomas Matulatis,^b Abhishek Kumar Gupta,^b Eli Zysman-Colman^{*b} and Sabine Laschat^{*a}

^a *Institut für Organische Chemie, Universität Stuttgart, Pfaffenwaldring 55, D-70569, Stuttgart, Germany. Email: sabine.laschat@oc.uni-stuttgart.de.*

^b *Organic Semiconductor Centre, EaStCHEM School of Chemistry, University of St Andrews, St Andrews, Fife, UK, KY16 9ST, Fax: +44-1334 463808; Tel: +44-1334 463826; E-mail: eli.zysman-colman@st-andrews.ac.uk.*

Author Contributions: J.A.K. conceived and supervised the project, performed the investigation of the mesomorphic / photophysical properties and wrote the first draft of the manuscript. B.S. performed the synthesis and T.M. and A.K.G. helped with photophysical investigations. E.Z.-C. and S.L. supervised the project and the manuscript preparation.

Table of Contents

1. General Methods	S2
1.1. Synthesis.....	S2
1.2. Quantum chemical calculations:	S3
1.3. Photophysical properties	S3
1.4. Mesomorphic properties.....	S5
2. Theoretical Calculations	S6
3. Synthesis	S7
4. NMR/ HRMS spectra and GPC traces	S12
5. Electrochemical Properties of the BON-LC	S27
6. Mesomorphic Properties	S28
7. Photophysical Properties.....	S30
8. Literature	S34

1. General Methods

1.1. Synthesis

Methods and Chemicals:

If not indicated otherwise, all chemicals were commercially available and have been used without further purification. Moisture and/ or air sensitive reagents were manipulated by Schlenk technique in flame dried glassware and in a MBraun glovebox. Dry toluene, CH_2Cl_2 and THF were distilled over sodium, CaH_2 and potassium, respectively. NMP, DMF, Xylene, Et_2O were dried over 4 Å molecular sieves and degassed by bubbling with N_2 .^[1] Petroleum ether, EtOAc and CH_2Cl_2 were distilled prior to use.

Thin layer chromatography (TLC):

Reaction monitoring and/or column chromatography was performed on TLC plates Alugram® Xtra SIL G/UV₂₅₄ from Macherey-Nagel as stationary phase with the indicated solvent mixture as mobile phase. Substance spots were identified by illuminating the plates with UV light (254 nm and 366 nm) or by immersing the plate in one of the following staining solutions followed by heating to 300 °C:

Cerium molybdate: $\text{Ce}(\text{NH}_4)_4(\text{NO}_3)_6$ (0.5 g) and $(\text{NH}_4)_6\text{Mo}_7\text{O}_{24} \cdot 4 \text{H}_2\text{O}$ (12 g) were dissolved in deionized H_2O (200 mL) and acidified with conc. H_2SO_4 (28 mL).

KMnO_4 : KMnO_4 (0.375 g), K_2CO_3 (2.5 g) and NaOH (0.1 g) were dissolved in deion. H_2O (50 mL).

Column chromatography:

Column chromatography was performed on Silica SiliFlash® P60 from Silicycle as stationary phase using the indicated solvent mixture as mobile phase. The columns were dry packed with silica and flushed with the indicated mobile phase. The crude products were applied on the column as a solution in the mobile phase if not indicated otherwise. Diameters (d) and lengths (l) of the silica was indicated in each procedure. Borylated silica for purification of boronic acids and boronic esters was prepared according to a literature procedure from silica gel and boric acid.^[2]

Gel Permeation Chromatography (GPC):

Analytical GPC analysis was performed on a Shimadzu Nexera system equipped with two serial Shimadzu ShimPack GPC 803 columns and THF as mobile phase. Preparative GPC was performed on BioBeads X-3 resin with THF as mobile phase (column dimensions: d x l = 3 cm x 150 cm).

Nuclear magnetic resonance spectroscopy:

^1H -NMR spectra were recorded at frequencies of 400 / 500 / 700 MHz, ^{11}B -NMR spectra were recorded at a frequency of 128 MHz, broadband decoupled ^{13}C -NMR spectra were recorded at frequencies of 101 / 126 / 176 MHz and ^{19}F spectra were recorded at a frequency of 376 MHz on Bruker ASCEND 400 / AVANCE 500 / AVANCE 700 spectrometers, respectively. Chemical shifts are given in parts per million (ppm) and referenced to the peak of the deuterated solvents if not indicated otherwise.^[3] Multiplicities are

given in Hz and abbreviated as follows: singlet (s), doublet (d), triplet (t), quartet (q), multiplet (m). COSY, HSQC, HMBC and NOESY spectra were utilized to assign the signals to the corresponding atoms.

Mass spectrometry:

High resolution mass spectra (HRMS) were measured on a Micromass GCT TOF-EI or a Micromass ZQ Single Quad ESI spectrometer.

Infrared Spectroscopy:

Infrared spectra were measured in solution on a Vektor 22 spectrometer by Bruker with a MKII Golden Gate Single Reflection Diamant ATR-System. The intensities of the absorption bands were classified as strong (s) and weak (w).

1.2. Quantum chemical calculations:

The calculations were performed with the Gaussian 16 revision C.01 suite^[4] for the density functional theory (DFT) calculations with the ORCA software package 5.0.3^[5,6] for double-hybrid DFT (DH-DFT). DFT was performed with the PBE0 functional^[7], 6-31G(d,p)^[8] and GD3BJ empirical dispersion in the gas phase. DH-DFT was performed using the wPBEP86 functional^[9] and cc-pVDZ basis set^[10] in the gas phase. Molecular orbital energies and isocountour plots were obtained based on the gas-phase ground state-optimized structures using the PBE0 functional. Excited-state calculations were performed using the double hybrid (DH) wPBEP86 functional and were we first optimized the ground state at the wPBEP86 level and vertical excitations to excited states were calculated based on this ground state-optimized structure. All calculations were submitted and processes using the Silico v5 software package^[11], which incorporates a number of publicly available software libraries, including: cclib^[12] for parsing of result files, VMD^[13] and Tachyon^[14] for 3D rendering and Open Babel^[15] and Pybel^[16] for the interconversion.

1.3. Photophysical properties

Sample preparation

Solution samples were prepared by dissolving the sample in the appropriate volume of HPLC grade or spectral grade solvent and eventually diluting with micropipettes to the appropriate concentration (0.01 – 0.02 mM). Degassed samples were prepared by 3 freeze-pump-thaw cycles. Thin Film samples were spin-coated from CHCl₃ solution (c = 10 - 40 mg mL⁻¹) on quartz or sapphire substrates on a Laurell WS-650-Mz-23NPPB spin coater at 1000 RPM and dried at ambient temperature for 30 min. Thick film samples were drop-casted from CHCl₃ solution (c = 10 - 20 mg mL⁻¹) on preheated (50 °C) quartz or sapphire substrates and dried at 50 °C for 10 min.

UV-Vis and Fluorescence spectroscopy:

Absorption spectra were recorded on a Shimadzu UV-2600 spectrophotometer in the indicated solvent. An integration sphere was used for recording the absorption spectra of spin coated or drop casted films. Extinction coefficients were determined by linear regression of the absorbance at five different

concentrations (absorbance = 0.629 – 1.534). Steady-state emission spectra were recorded on a FS5 spectrofluorometer from Edinburgh instruments in the indicated solvent ($c = 0.02$ mM) or as a drop-caste / spin-coated film.

Steady-State and Time-Resolved Photoluminescence Measurements

Solution samples were investigated using a FS-5 instrument by Edinburgh Instruments equipped with a xenon lamp and an EPL-375 picosecond laser source ($\lambda_{\text{exc}} = 375$ nm) for steady state and time resolved measurements, respectively. Film samples were investigated on a FLS-980 instrument by Edinburgh Instruments equipped with a xenon lamp and a laser diode ($\lambda_{\text{exc}} = 379$ nm) and a Picoquant 800-D driver driver for steady-state and time-resolved measurements, respectively. The film samples were mounted onto a cold finger cryostat driven by a Mercury ITC controller from Oxford instruments ($T = 77 - 310$ K) for variable temperature measurements under air and vacuum. Time correlated single photon counting (TCSPC) and multi-channel scaling (MCS) experiments were conducted to record photoluminescence decays in the ns and μs regime, respectively. The corresponding decay curves were fitted to (multi)exponential functions according to the least squares method to determine the lifetimes of the excited states. If applicable, amplitude average lifetimes τ_{avg} were calculated for multiexponential decays.^[17]

Photoluminescence Quantum Yields (PLQYs):

Solution PLQYs were determined utilizing the optical dilute method^[18] in air saturated and degassed toluene solutions using quinine sulfate in 0.5 M H_2SO_4 ($\Phi_{\text{r}} = 54.6\%$ ^[19]) as a standard. Four samples with absorptions of ca. 0.05, 0.0375, 0.025 and 0.0125 were prepared and their PLQYs, Φ_{PL} , were determined using the equation $\Phi_{\text{PL}} = \Phi_{\text{r}}(A_{\text{r}}/A_{\text{s}})(I_{\text{s}}/I_{\text{r}})(n_{\text{s}}/n_{\text{r}})^2$, where A_{r} and A_{s} are absorption of reference and sample, I_{r} and I_{s} are emission intensity of reference and sample and n_{r} and n_{s} are the refractive indices of reference and sample solvent, respectively. Film PLQYs were determined using a FS-5 spectrometer from Edinburgh Instruments equipped with a calibrated integration sphere ($\Delta\Phi_{\text{PL}} = 5\%$) as an average of 3 measurements under air or N_2 atmosphere.

ΔE_{ST} measurements:

The singlet and triplet state energies were determined from the onset values of the prompt fluorescence and phosphorescence spectra at 77 K in glassy toluene. The singlet-triplet energy gap (ΔE_{ST}) was estimated from the difference in energy of the prompt fluorescence and phosphorescence spectra. Prompt fluorescence spectra were measured from 1 ns after photoexcitation with an iCCD exposure time of 100 ns. Phosphorescence spectra were measured from 1 ms after photoexcitation with an iCCD exposure time of 8.5 ms. The samples were excited by a femtosecond laser emitting at 343 nm (Orpheus-N, model: SP-06-200-PP). Emission from the samples was focused onto a spectrograph (Chromex imaging, 250is spectrograph) and detected on a sensitive gated iCCD camera (Stanford Computer Optics, 4Picos) having sub-nanosecond resolution.

Electrochemical Measurements:

Cyclic Voltammetry (CV) and Differential Pulse Voltammetry (DPV) analysis were performed on a CHIE620E potentiostat from CH Instruments. All measurements were performed in 0.1 M electrolytes of tetrabutylammonium hexafluorophosphate [$n\text{Bu}_4\text{N}]\text{PF}_6$ in CH_2Cl_2 degassed by sparging with CH_2Cl_2 saturated N_2 gas. The measurement cell consisted of an Ag/Ag^+ reference electrode, a glassy carbon working electrode and a platinum wire as counter electrode. The redox potentials are reported relative to a saturated calomel electrode (SCE) utilizing the ferrocene/ferrocenium (Fc/Fc^+) redox couple (sublimed, 0.46 V vs SCE) as internal standard.^[20] The HOMO and LUMO values were extracted from the anodic / cathodic DPV peak potentials according to $E_{\text{HOMO/LUMO}} = - (E_{\text{ox}} / E_{\text{red}} + 4.8) \text{ eV}$.^[21]

1.4. Mesomorphic properties

Differential Scanning Calorimetry (DSC):

DSC measurements were performed on a DSC822^e by Mettler Toledo in standardized 40 μL aluminum crucibles and evaluated with the software STAR^e 14.0. Phase transition temperatures are given as onsets of the corresponding peaks.

Polarizing Optical Microscopy (POM):

A polarizing optical microscope Olympus BX50 equipped with a variable temperature sample holder LTS350 (control unit: TP39 and LNP, $\Delta T = \pm 1 \text{ K}$) by Linkam Scientific was used to investigate the mesomorphic properties of our compounds. Micrographs were taken with a Zeiss Axiocam 105 color camera module and the software ZEN core. The samples were investigated on regular glass slides and in polyimide coated cells.

Wide (WAXS) and small angle (SAXS) X-ray diffraction:

For X-ray diffraction studies, the samples were sealed in glass capillaries supplied by Hilgenberg GmbH (external diameter of 0.7 mm, wall thickness 0.01 mm). Two-dimensional X-ray diffraction (2D-WAXS and 2D-SAXS) studies were carried out on a Bruker AXS Nanostar C equipped with a ceramic tube generator (CuK_α radiation, $\lambda = 1.5405 \text{ \AA}$, 1500 W) and a Bruker Vantec 500 detector. The diffractograms were processed using SAXS software and calibrated to the diffraction pattern of silver behenate at 25 $^\circ\text{C}$.

2. Theoretical Calculations

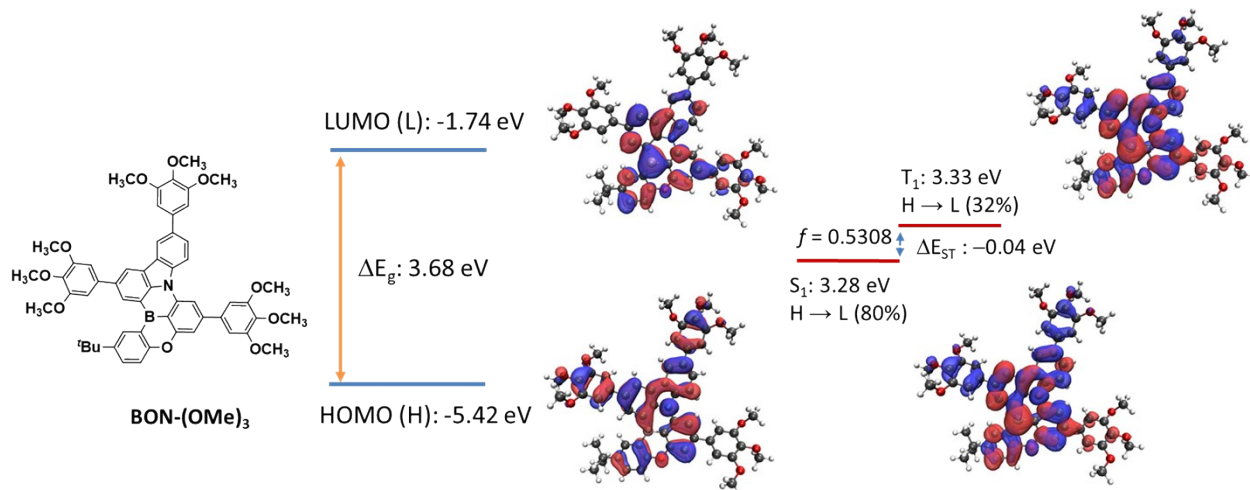


Figure S1: Isocontour plots of the HOMO and LUMO orbitals (isovalue = 0.02), frontier orbitals energy diagram, difference density plots (isovalue = 0.02) calculated at the PBE0/6-31G(d,p) level in vacuum by using TDA-DFT methodology and energies of the lowest singlet and triplet excite states for **BON(OMe)₃** calculated at DH DFT using the wpBEPP86 functional and cc-pVDZ basis set in gas phase.

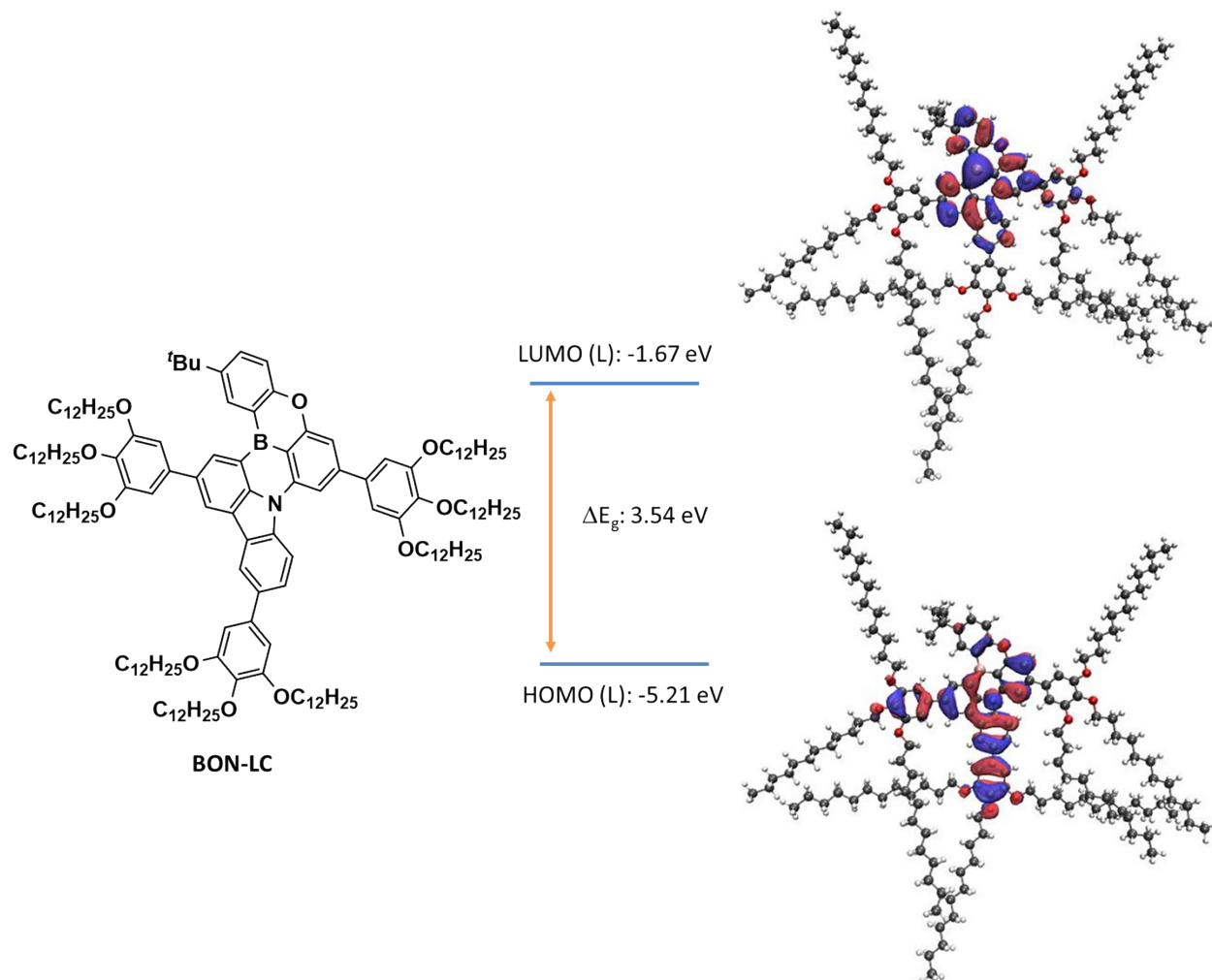
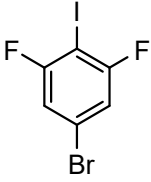
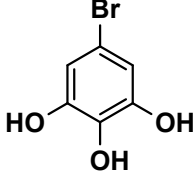
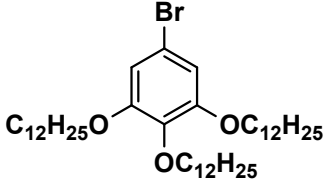
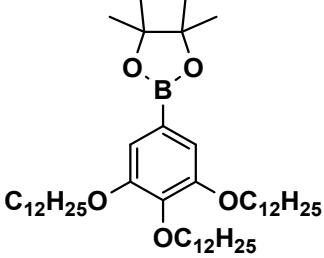


Figure S2: Isocontour plots of the HOMO and LUMO orbitals, frontier orbitals ((isovalue = 0.02), energy diagram, and difference density plots for **BON-LC** calculated at the TDA-DFT-PBE0/6-31G(d,p) level in vacuum.

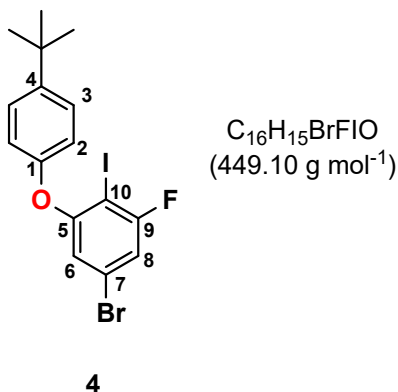
3. Synthesis

The following literature known compounds were prepared according to literature procedures from commercially available starting materials:

Table S1: Literature known compounds prepared for this study analog to the corresponding references.

	$C_6H_2BrF_2I$ (318.89 g mol ⁻¹)	Synthesis from 1-bromo-3,5-difluorobenzene according to Ref. [11]. ^[22]
3		
	$C_6H_5BrO_3$ (205.01 g mol ⁻¹)	Synthesis from 1-bromo-3,4,5-trimethoxybenzene according to Ref. [9]. ^[23]
7		
	$C_{42}H_{77}BrO_3$ (709.98 g mol ⁻¹)	Synthesis from 7 according to Ref. [10]. ^[24]
8		
	$C_{48}H_{89}BO_5$ (757.04 g mol ⁻¹)	Synthesis from 8 according to Ref. [9]. ^[23]
9		

5-bromo-1-(4-(tert-butyl)phenoxy)-3-fluoro-2-iodobenzene (4):



Fluorobenzene **3** (4.00 g, 12.54 mmol, 1.0 equiv.), 4-*tert*-butylphenol (1.88 g, 12.54 mmol, 1.0 equiv.) and Cs₂CO₃ (4.09 g, 12.54 mmol, 1.0 equiv.) were suspended in anhydrous DMF (40 mL) and stirred at 80 °C for 72 h. After cooling to r.t., deionized water (100 mL) was added and the mixture was extracted with EtOAc (3 × 100 mL). The combined organic phase was washed with brine (100 mL) and dried over MgSO₄. Removal of the solvent under reduced pressure and purification via column chromatography (Eluent: PE) afforded the desired product as colourless solid (2.78 g, 6.2 mmol, 49%).

¹H-NMR (400 MHz, CDCl₃): δ = 1.34 (s, 9H, CH₃), 6.70 (d, J = 1.8 Hz, 1H, 6-H), 6.95–7.00 (m, 3H, 2-H, 8-H), 7.38–7.43 (m, 2H, 3-H) ppm.

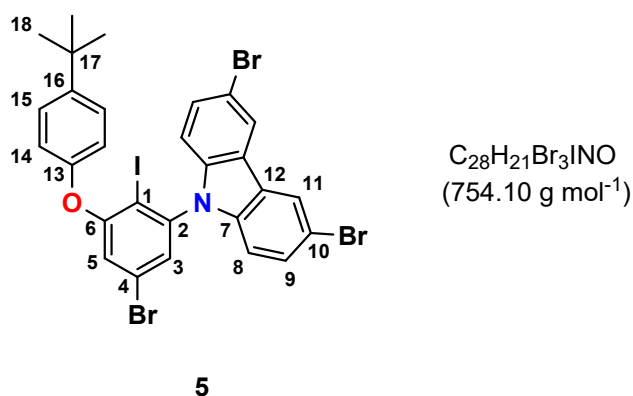
¹³C-NMR (126 MHz, CDCl₃): δ = 31.59 (s, CH₃), 34.63 (s, C(CH₃)₃), 75.21 (d, J = 27.6 Hz, C-10), 113.77 (d, J = 27.6 Hz, C-8), 116.27 (d, J = 3.1 Hz, C-6), 119.29 (s, C-2), 122.89 (d, J = 11.9 Hz, C-7) 127.18 (s, C-3), 148.11 (s, C-4), 153.13 (s, C-1), 159.70 (d, J = 6.2 Hz, C-5), 163.02 (d, J = 248.4 Hz, C-9) ppm.

¹⁹F-NMR (376 MHz, CDCl₃): δ = -89.78 (d, J = 7.1 Hz) ppm.

FT-IR(ATR) $\tilde{\nu}$ = 2961.87 (w), 1447.18 (w), 1292.83 (w), 1268.02 (w), 550.55 (w), 1574.45 (s), 1507.18 (s), 1401.26 (s), 1214.94 (s), 1026.14 (s), 861.43 (s), 831.05 (s) cm⁻¹.

HRMS (EI) m/z for C₁₆H₁₅BrFIO⁺ calculated: 450.9349 [M+H], found: 450.9345

3,6-dibromo-9-(5-bromo-3-(4-(tert-butyl)phenoxy)-2-iodophenyl)-9H-carbazole (5):



The precursor **4** (2.2 g, 4.9 mmol, 1.0 equiv.), dibromocarbazole (1.75 g, 5.4 mmol, 1.1 equiv.) and Cs₂CO₃ (1.76 g, 5.4 mmol, 1.1 equiv.) were suspended in anhydrous DMF (20 mL) and stirred at 80 °C for 72 h. After cooling to r.t., deion. H₂O (100 mL) was added and the mixture was extracted with EtOAc (3 × 100 mL). The combined organic phase was washed with deion. H₂O (3 × 100 mL), brine (3 × 100 mL) and dried over MgSO₄. Removal of the volatiles under reduced pressure and subsequent column chromatography on silica (gradient, PE to PE : CH₂Cl₂ = 20 : 1) afforded **7** as colourless solid (2.95 g, 3.91 mmol, 80%).

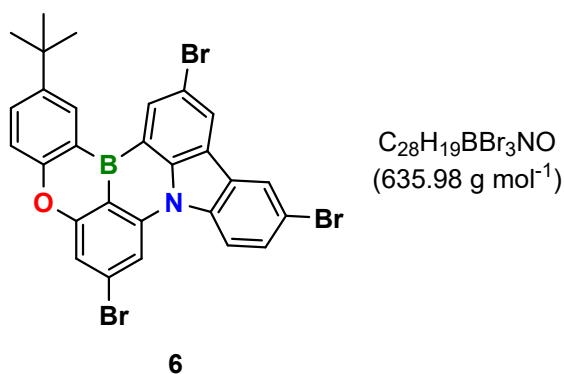
¹H NMR (500 MHz, CDCl₃): δ = 1.37 (s, 9H, 18-H), 6.99 (d, *J* = 8.6 Hz, 2H, 8-H), 7.04 – 7.09 (m, 3H, 14-H and 5-H or 3-H), 7.27 (d, *J* = 2.1 Hz, 1H, 5-H or 3-H), 7.45 – 7.49 (m, 2H, 15-H), 7.54 (dd, *J* = 8.6, 1.9 Hz, 2H, 9-H), 8.22 (d, *J* = 1.9 Hz, 2H, 11-H).

¹³C NMR (101 MHz, CDCl₃): δ = 31.6 (C-18), 34.7 (C-17), 91.8 (C-1), 112.1 (C-8), 113.8 (C-10), 119.5 (C-14), 120.5 (C-5 or C-3), 123.5 (C-4), 123.6 (C-11), 124.2 (C-12), 127.39 (C-15), 127.42 (C-5 or C-3), 129.8 (C-9), 139.5 (C-7), 142.4 (C-2), 148.5 (C-16), 152.9 (C-13), 160.5 (C-6).

FT-IR (ATR) $\tilde{\nu}$ = 2961.75 (w), 1363.60 (w), 1108.39 (w), 1316.50 (w), 1172.15 (w), 1403.30 (w), 827.85 (w), 1022.24 (w), 732.30 (w), 546.62 (w), 1562.70 (s), 1505.79 (s), 1469.56 (s), 1434.26 (s), 1402.91 (s), 1280.57 (s), 1255.88 (s), 1228.76 (s), 908.91 (s) cm⁻¹

HRMS (APCI) *m/z* for C₂₈H₂₁Br₃INO⁺ calculated: 753.8272, found: 753.8278

7,11,14-tribromo-2-(tert-butyl)-5-oxa-8b-aza-15b-borabenz[a]naphtho[1,2,3-hi]aceanthrylene (6):



Under nitrogen atmosphere **5** (500 mg, 663.04 μmol, 1 equiv.) was dissolved in xylene (5 mL) and the reaction mixture was cooled to -40 °C. Then, *n*-BuLi (0.29 mL, 729.35 μmol, 2.5 M in hexane, 1.1 equiv.) was quickly added. The reaction mixture was warmed up to r.t and stirred at r.t. for 1 h whereby the formation of a colourless precipitate could be observed. Then, BBr₃ (0.07 mL, 795.65 μmol, 1.2 equiv.) was added to the reaction mixture at 0 °C and the precipitate redissolved. After stirring for at r.t. for 30 min, diisopropylethylamine (0.24 mL, 1.46 mmol, 2.2 equiv.) was added, the mixture was heated to 140 °C and stirred for 18 h. After that, deionized water (10 mL) and PE (5 mL) were added to quench the reaction. The formed precipitate was treated in an ultrasonic bath for 5 min and then filtered off. The filter cake was

washed with deionized H₂O, MeOH, EtOH and PE (50 mL each) to afford the product as yellow solid (203 mg, 319.2 μmol, 48%).

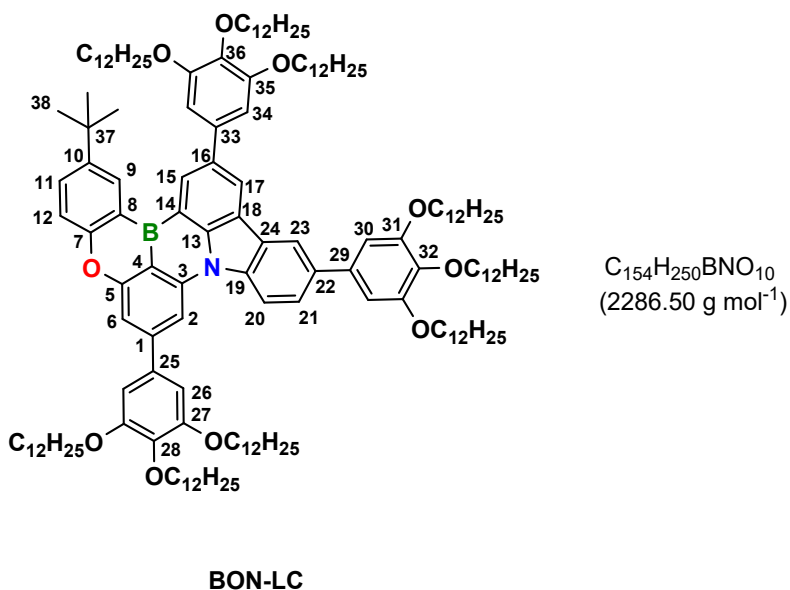
¹H-NMR (400 MHz, CDCl₃, 323 K): δ = 1.56 (s, 9H), 7.51 (s, 1H), 7.52 (d, *J* = 7.9 Hz, 1H), 7.75 (dd, *J* = 8.9 Hz, 2.2 Hz, 1H), 7.86 (dd, *J* = 8.7 Hz, 2.5 Hz, 1H), 8.13 (d, *J* = 8.9 Hz, 1H), 8.15 (d, *J* = 1.5 Hz, 1H), 8.23 (d, *J* = 2.1 Hz, 1H), 8.38 (d, *J* = 1.9 Hz, 1H), 8.66 (d, *J* = 2.6 Hz, 1H), 8.87 (d, *J* = 1.9 Hz, 1H) ppm.

FT-IR (ATR) $\tilde{\nu}$ = 2954.43 (w), 1738.57 (w), 1577.86 (w), 1567.08 (w), 1388.45 (w), 1247.02 (w), 1231.82 (w), 1210.31 (w), 821.93 (w), 732.89 (w), 569.89 (w) cm⁻¹.

HRMS (EI) *m/z* for C₂₈H₁₉BBr₃NO⁺ calculated: 637.9102 [M+H]⁺, found: 637.9105

Please note: The product **8** was not sufficiently soluble for ¹³C and 2D NMR analysis. The identity and purity were estimated from HRMS and ¹H-NMR analysis, respectively.

2-(tert-butyl)-7,11,14-tris(3,4,5-tris(dodecyloxy)phenyl)-5-oxa-8b-aza-15b-borabenz[a]naphtho[1,2,3-hi]aceanthrylene (BON-LC):



The aromatic core **6** (30 mg, 47 μmol, 1 equiv.), Cs₂CO₃ (72 mg, 236 μmol, 5 equiv.) and the pinacolborolane **9** (125 mg, 165 μmol, 3.5 equiv.) were suspended in a mixture of toluene (3 mL), EtOH (1.5 mL) and water (1.5 mL) and degassed for 30 min prior to adding Pd(PPh₃)₄ (8 mg, 7 μmol, 0.15 equiv.). The mixture was subsequently heated to 105 °C and stirred for 18 h. Then, the reaction mixture was cooled to r.t, diluted with toluene (20 mL) and the phases were separated. The organic phase was washed with brine (1 × 10 mL) and dried over MgSO₄. Column chromatography on silica gel (gradient: PE to PE : DCM = 2 : 1) and subsequent purification via preparative GPC afforded **BON-LC** as yellow wax (45 mg, 47 μmol, 42%).

$^1\text{H-NMR}$ (700 MHz, CD_2Cl_2): δ = 0.70–0.89 (m, 27H, CH_3), 1.11–1.37 (m, 144H, CH_2), 1.39–1.54 (m, 30H, CH_2 and 38-H), 1.66–1.84 (m, 18H, O CH_2CH_2), 3.91–4.08 (m, 18H, OCH_2), 6.88 (s, 2H, 26-H), 6.91 (s, 2H, 30-H or 34-H), 6.97 (s, 2H, 30-H or 34-H), 7.35 (s, 1H, 6-H), 7.37 (d, J = 8.7 Hz, 1H, 12-H), 7.60–7.81 (m, 2H, 11-H and 20-H or 21-H), 8.19 (s, 1H, 2-H), 8.30 (d, J = 8.8 Hz, 1H, 20-H or 21-H), 8.33 (s, 1H, 23-H), 8.50 (s, 1H, 15-H or 17-H), 8.72 (s, 1H, 9-H), 8.90 (s, 1H, 15-H or 17-H) ppm.

$^{13}\text{C-NMR}$ (176 MHz, CD_2Cl_2): δ = 13.91, 13.92, 22.72, 22.75, 26.25, 26.28, 26.29, 26.31, 29.4, 29.5, 29.57, 29.58, 29.65, 29.68, 29.73, 29.75, 29.76, 29.78, 29.80, 29.84, 29.86, 29.87, 30.48, 30.53, 31.5, 31.97, 32.00, 34.5, 69.2, 69.3, 73.49, 73.51, 73.6, 105.6, 105.7, 106.1, 106.5, 108.0, 114.6, 117.4, 117.5, 119.1, 121.5, 122.4, 122.6, 124.3, 126.2, 127.3, 130.4, 131.3, 131.7, 135.5, 135.9, 136.0, 136.1, 136.9, 137.6, 137.8, 138.7, 139.2, 142.3, 143.2, 145.1, 147.6, 153.61, 153.62, 153.8, 157.9, 159.3 ppm.

$^{11}\text{B-NMR}$ (128 MHz, C_6D_6): δ = 27.7 ppm.

FT-IR (ATR) $\tilde{\nu}$ = 2954 (s), 2921 (s), 2853 (s), 1618 (w), 1584 (w), 1570 (w), 1542 (w), 1505 (w), 1467 (w), 1433 (w), 1411 (w), 1380 (w), 1326 (w), 1271 (w), 1237 (s), 1188 (w), 1113 (s), 1012 (w), 956 (w), 887 (w), 816 (w), 755 (w), 723 (w), 625 (w), 575 (w) cm^{-1} .

HRMS (APCI) m/z for $\text{C}_{154}\text{H}_{250}\text{BNO}_{10}^+$ calculated: 2286.9297 $[\text{M}+\text{H}]^+$ found: 2286.9291.

4. NMR/ HRMS spectra and GPC traces

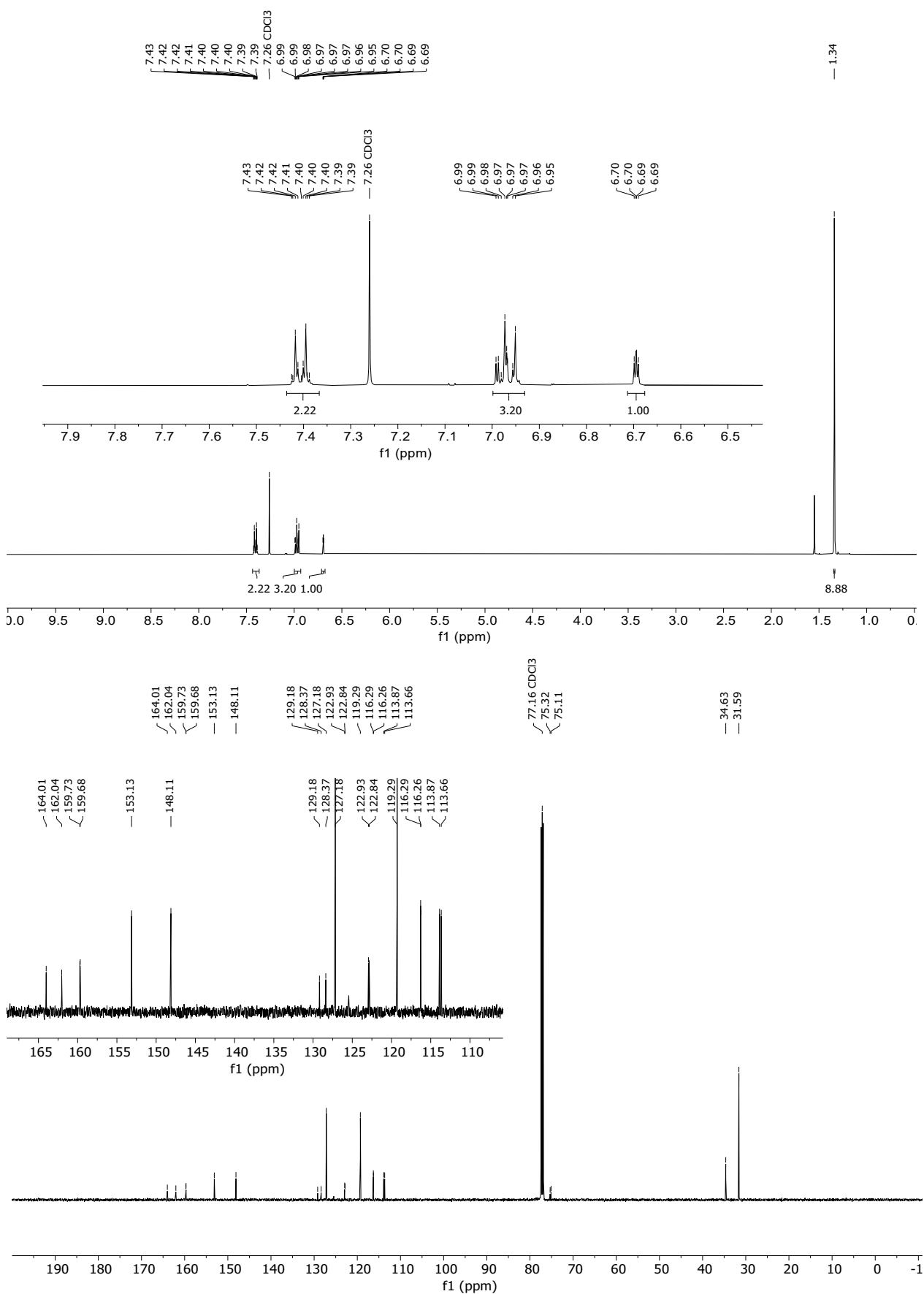


Figure S3: ¹H NMR spectrum (top, 400 MHz, inset shows aromatic region in detail) and ¹³C NMR

spectrum (bottom, 126 MHz) of **4** in CDCl₃.

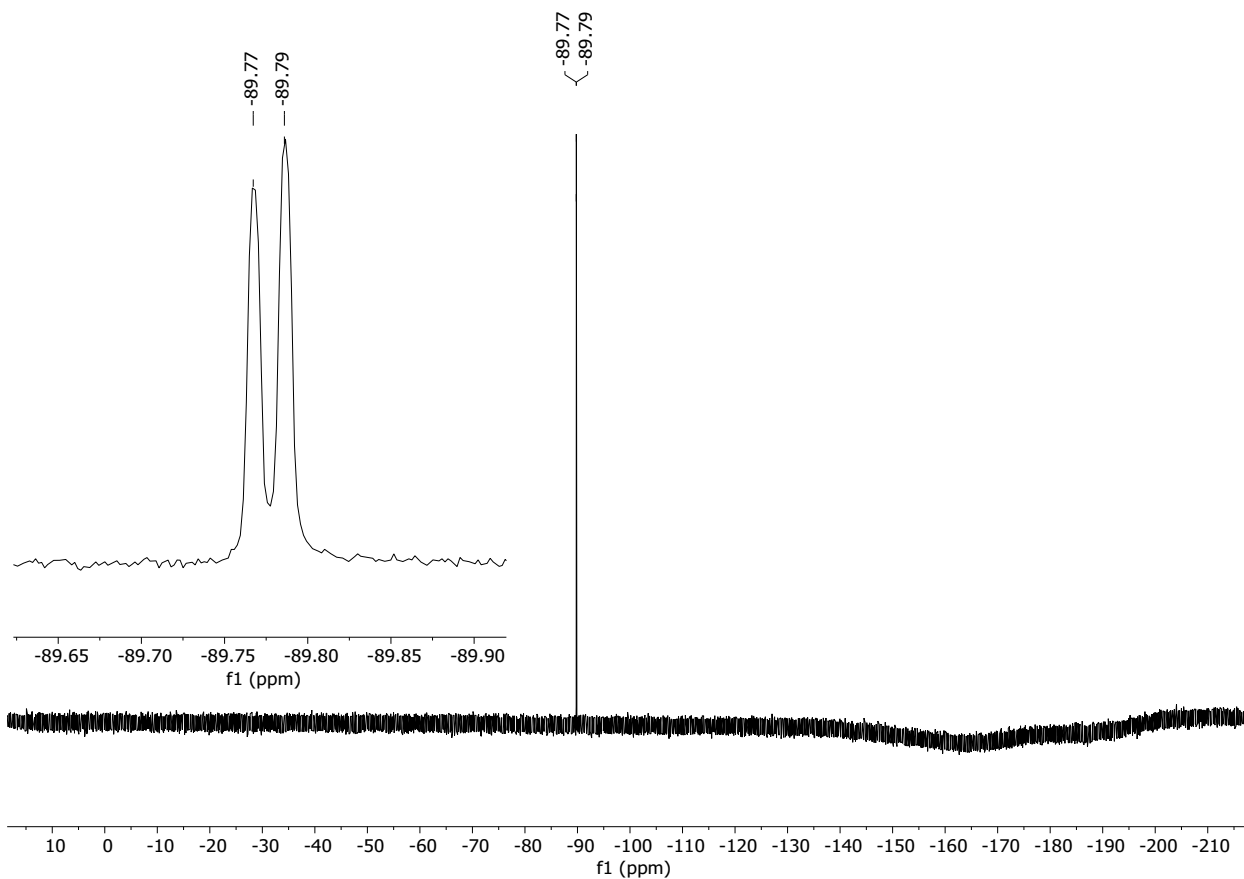


Figure S4: ¹⁹F NMR spectrum (top, 376 MHz, inset signal in detail) of **4** in CDCl₃.

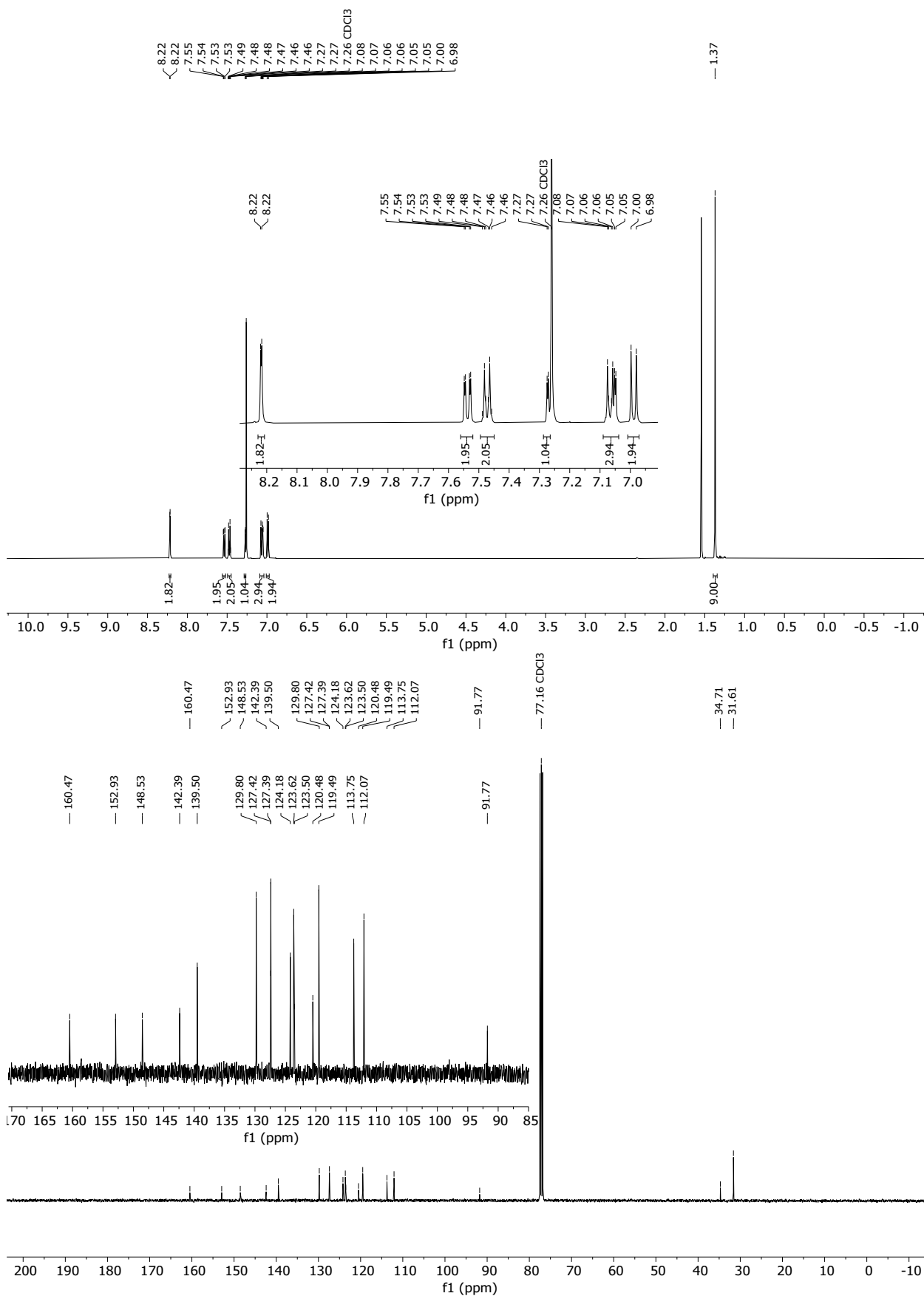


Figure S5: ¹H NMR spectrum (top, 500 MHz, inset shows aromatic region in detail) and ¹³C NMR spectrum (bottom, 101 MHz) of **5** in CDCl₃.

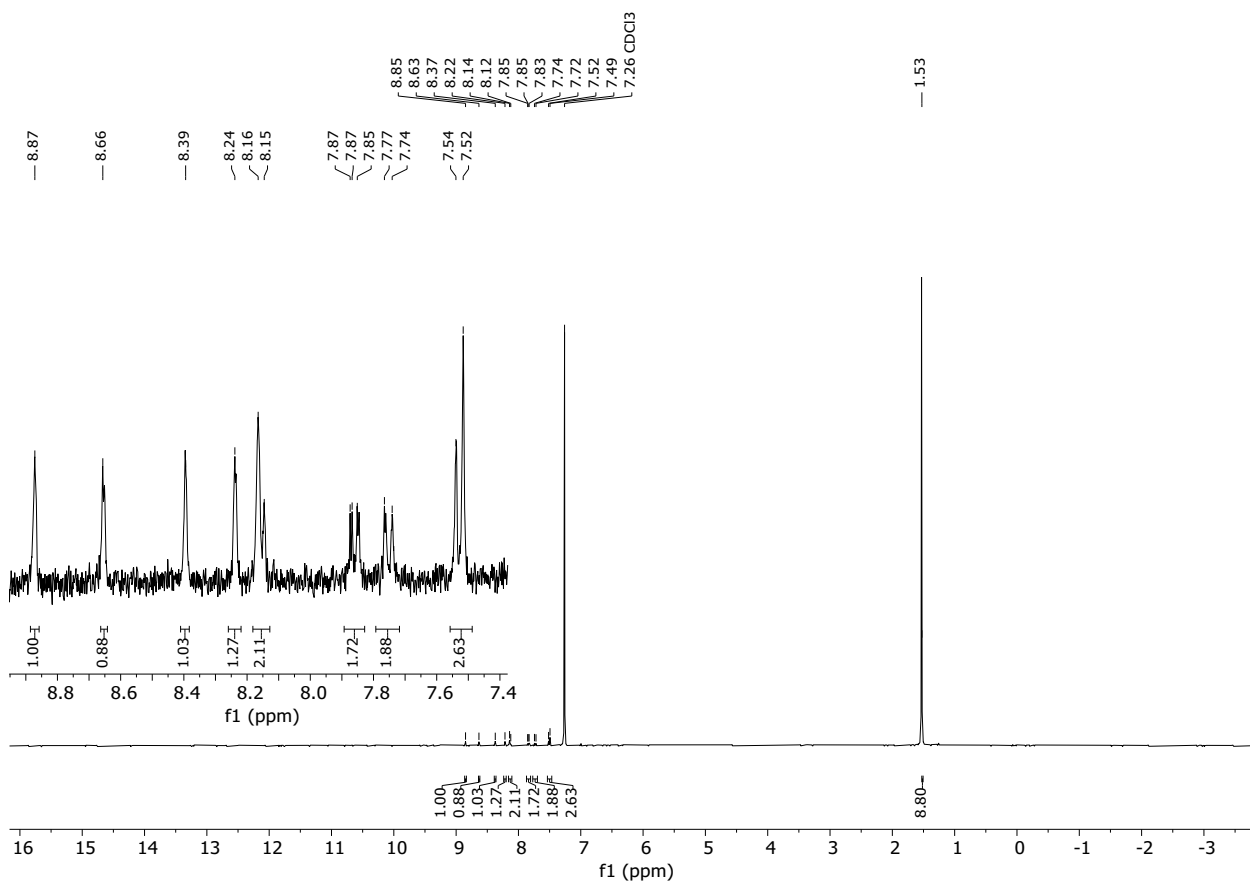


Figure S6: ^1H NMR spectrum (400 MHz, inset shows aromatic region in detail) of **6** in CDCl_3 .

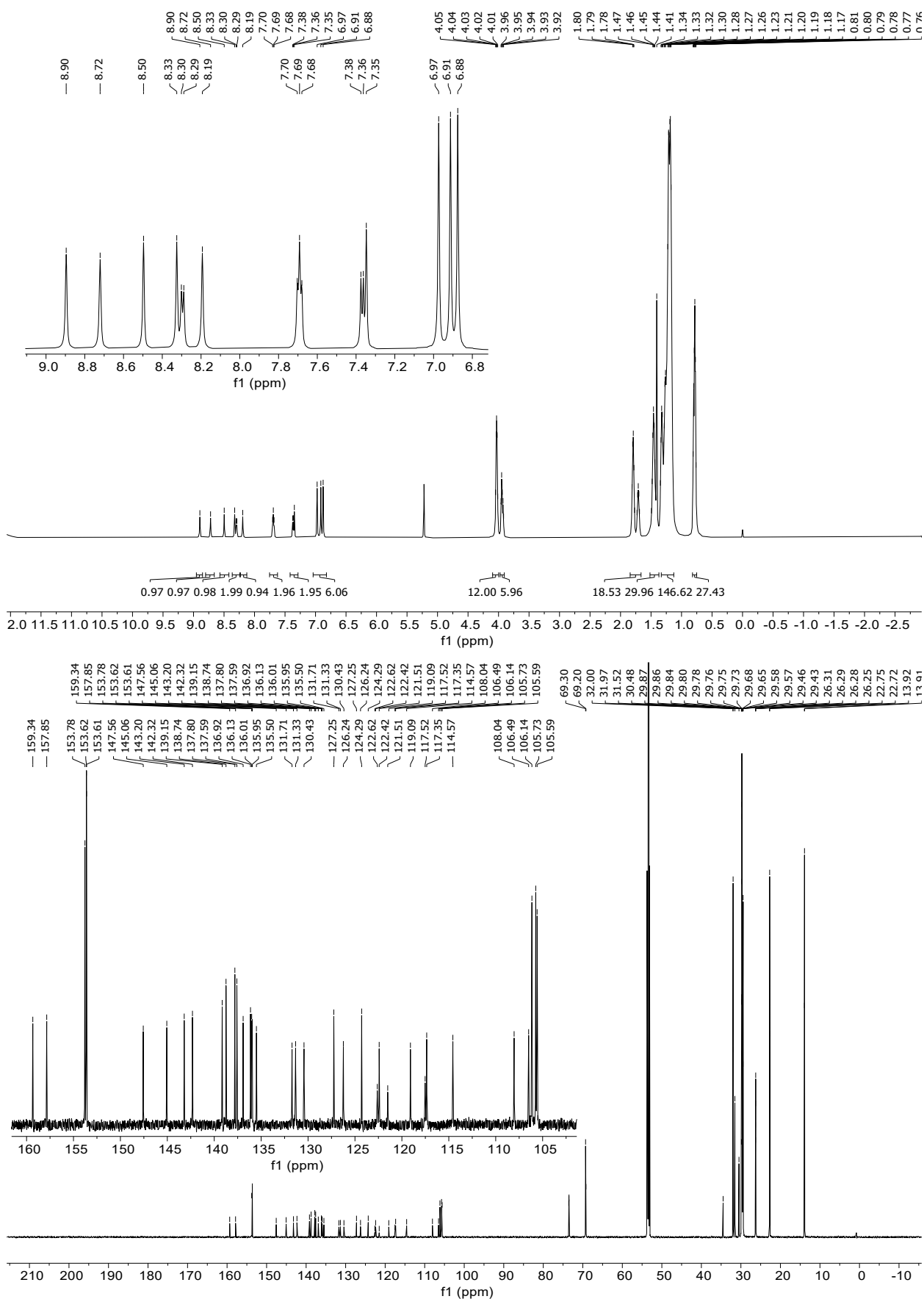


Figure S7: ¹H NMR spectrum (top, 700 MHz, inset shows aromatic region in detail) and ¹³C NMR spectrum (bottom, 176 MHz) of **BON-LC** in CD₂Cl₂.

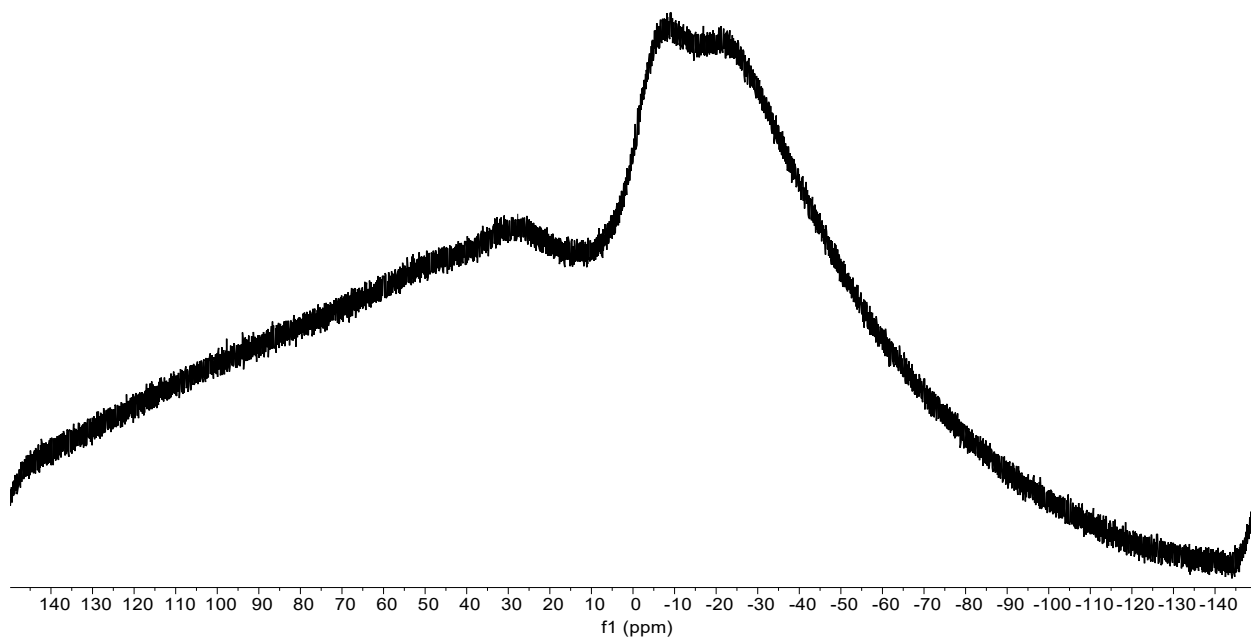


Figure S8: ^{11}B NMR spectrum (128 MHz) of **BON-LC** in C_6D_6 at 343 K.

File :C:\MSDCHEM\1\DATA\SUNMET-BUR-066-FILTRIERT.D
Operator :
Acquired : 13 Jul 2021 8:40 using AcqMethod DEFAULTTEST.M
Instrument : Instrument #1
Sample Name: BUR-066-filtriert
Misc Info :
Vial Number: 1

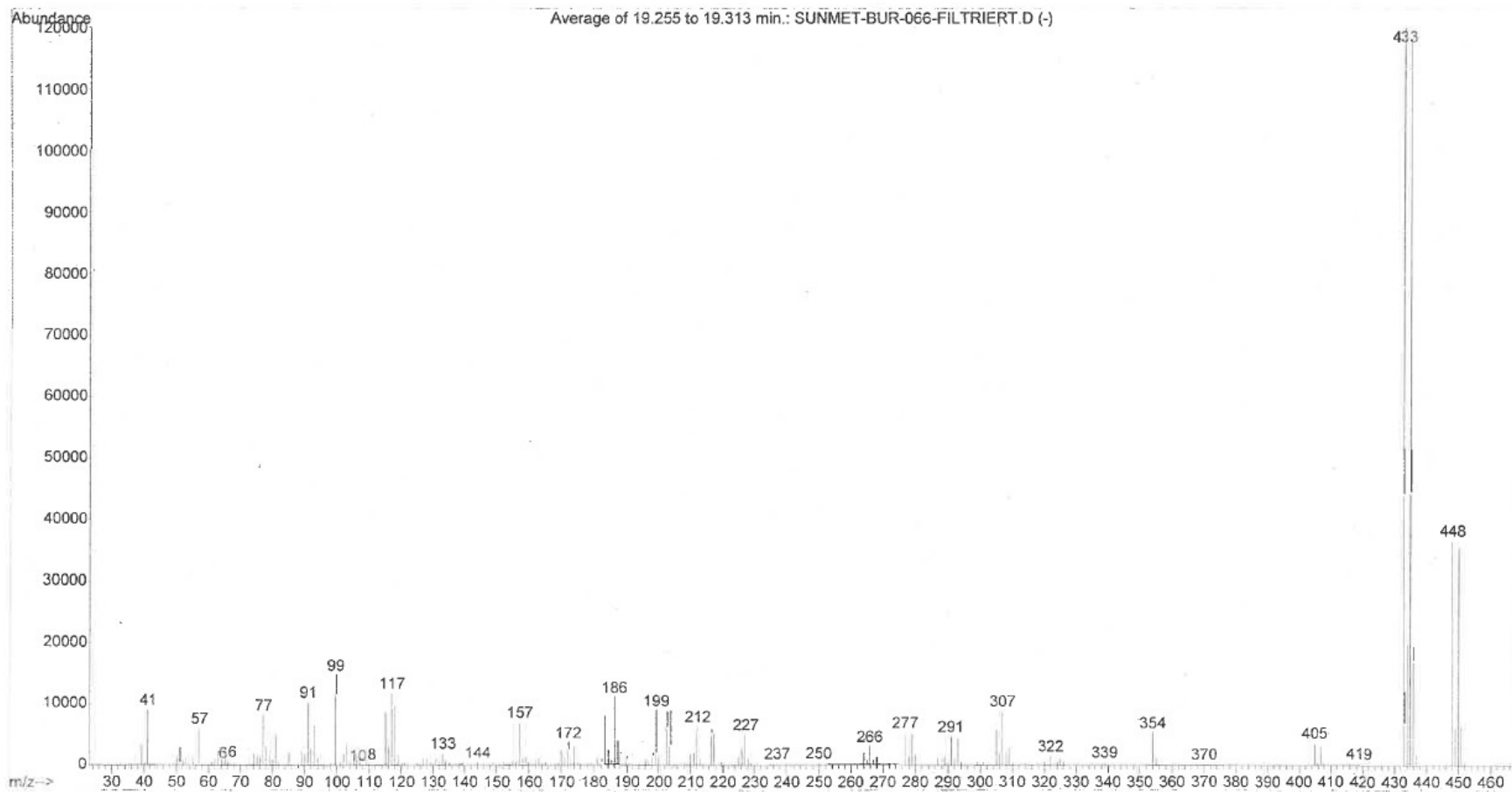


Figure S9: Low resolution mass spectrum of 4.

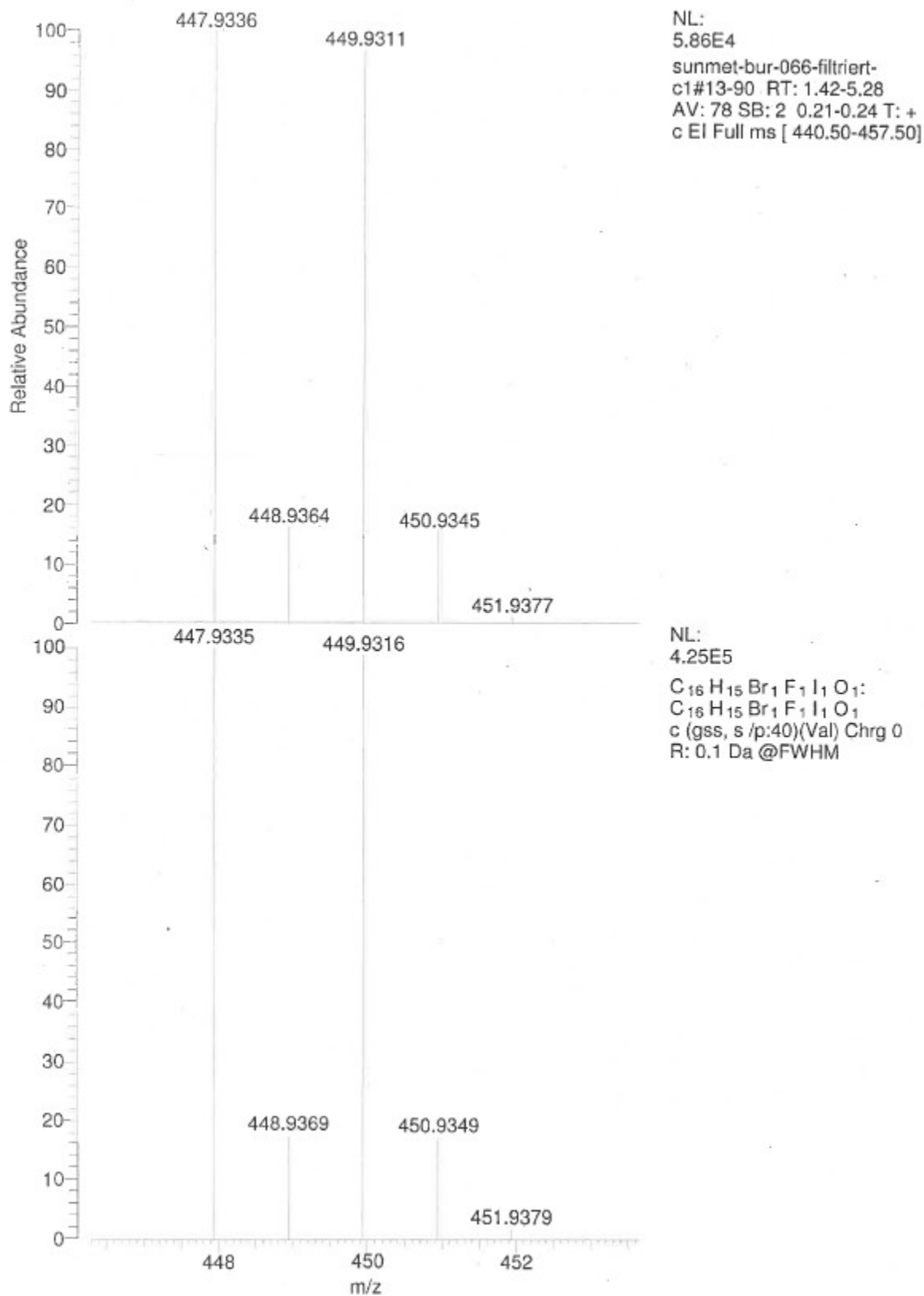


Figure S10: High resolution mass spectrum of 4.

Sönmez

Massenspektrometrie - Universität Stuttgart

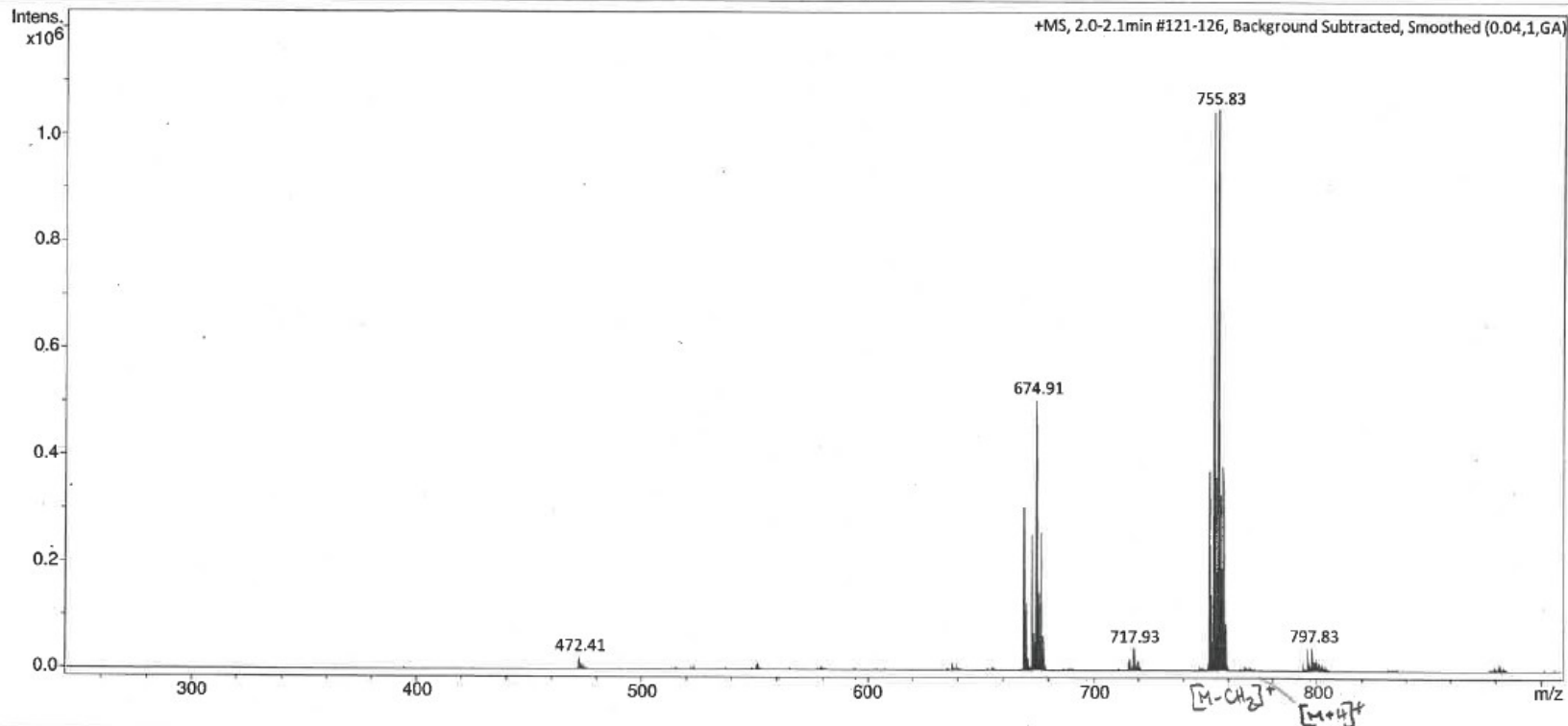
Analysis Info

Analysis Name Sönmez-BUR-069-vollchar_1_01_35418.d
Method tune-wide-oktober-2019.m
Sample Name Sönmez-BUR-069-vollchar
Comment

Acquisition Date 10/26/2021 3:15:46 PM
Operator BDAL@DE
Instrument micrOTOF-Q 228888.00043

Acquisition Parameter

Source Type	APCI	Ion Polarity	Positive	Set Nebulizer	1.7 Bar
Focus	Not active	Set Capillary	4500 V	Set Dry Heater	300 °C
Scan Begin	250 m/z	Set End Plate Offset	-500 V	Set Dry Gas	5.0 l/min
Scan End	3000 m/z	Set Collision Cell RF	500.0 Vpp	Set Divert Valve	Waste



Bruker Compass DataAnalysis 4.2

printed: 10/26/2021 3:27:52 PM

Page 1 of 1

Figure S11: Low resolution mass spectrum of 5.

Massenspektrometrie - Universität Stuttgart

Analysis Info

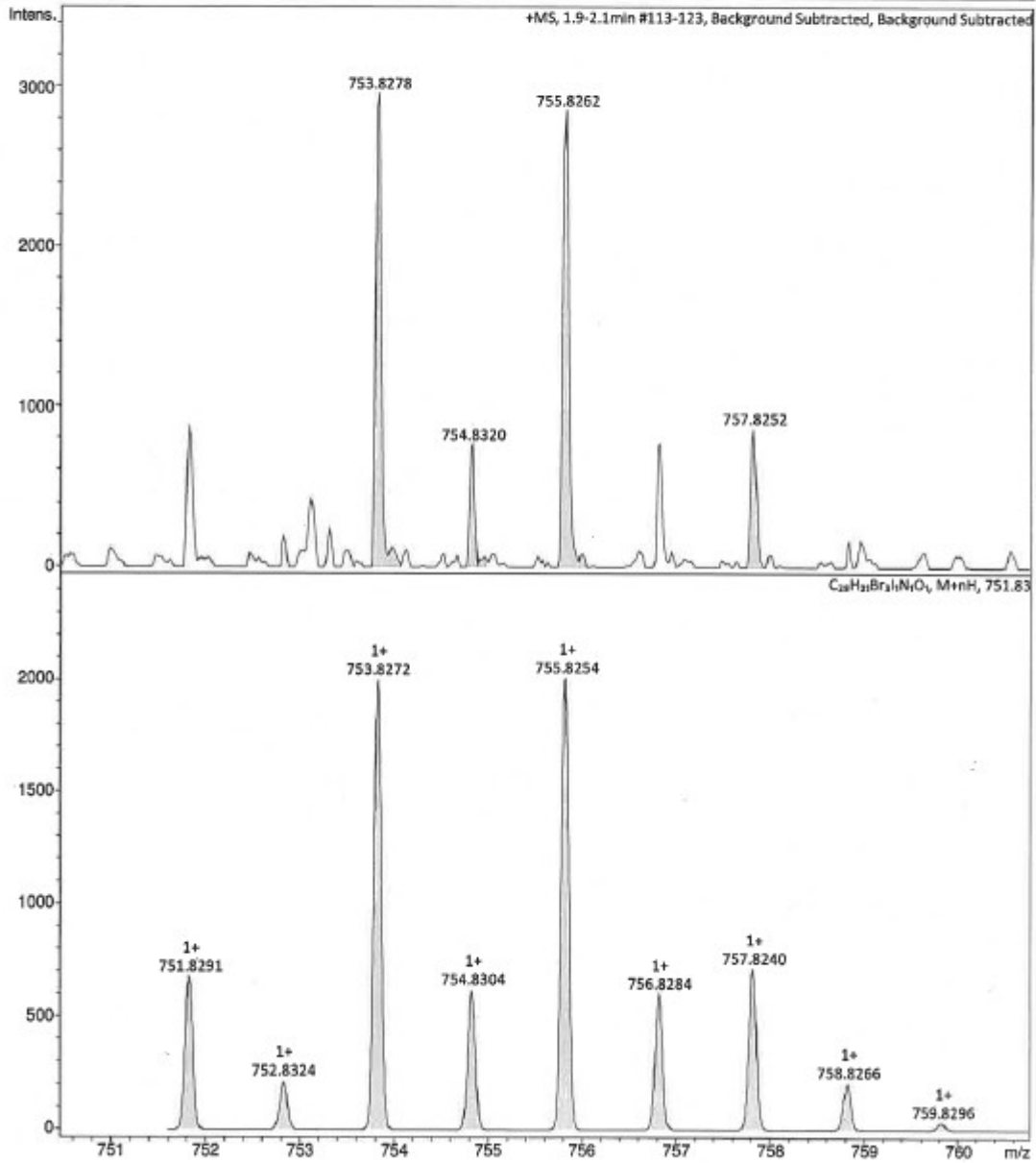
Analysis Name Soenmez-BUR-069-Vollich_3_01_33447.d
Method tune-wide-oktober-2019.m
Sample Name Soenmez-BUR-069-Vollich
Comment

Acquisition Date 7/23/2021 9:31:51 AM

Operator BDAL@DE
Instrument micrOTOF-Q 228888.00
043

Acquisition Parameter

Source Type	ESI	Ion Polarity	Positive	Set Nebulizer	0.4 Bar
Focus	Not active	Set Capillary	4500 V	Set Dry Heater	200 °C
Scan Begin	250 m/z	Set End Plate Offset	-500 V	Set Dry Gas	4.0 l/min
Scan End	3000 m/z	Set Collision Cell RF	500.0 Vpp	Set Divert Valve	Waste



Bruker Compass DataAnalysis 4.2

printed: 7/23/2021 10:11:23 AM

Page 1 of 1

Figure S12: High resolution mass spectrum of 5.

D:\Xcalibur\data\soenmez-bur-071
El positiv-Ion, 70eV

Tquelle=170°C
Tprobe=340°C

7/26/2021 1:27:41 PM

BUR-071
Soenmez

soenmez-bur-071 #228-306 RT: 18.29-24.52 AV: 79 SB: 8 0.38-0.93 NL: 1.20E5
T: + c EI Full ms [24.50-850.50]

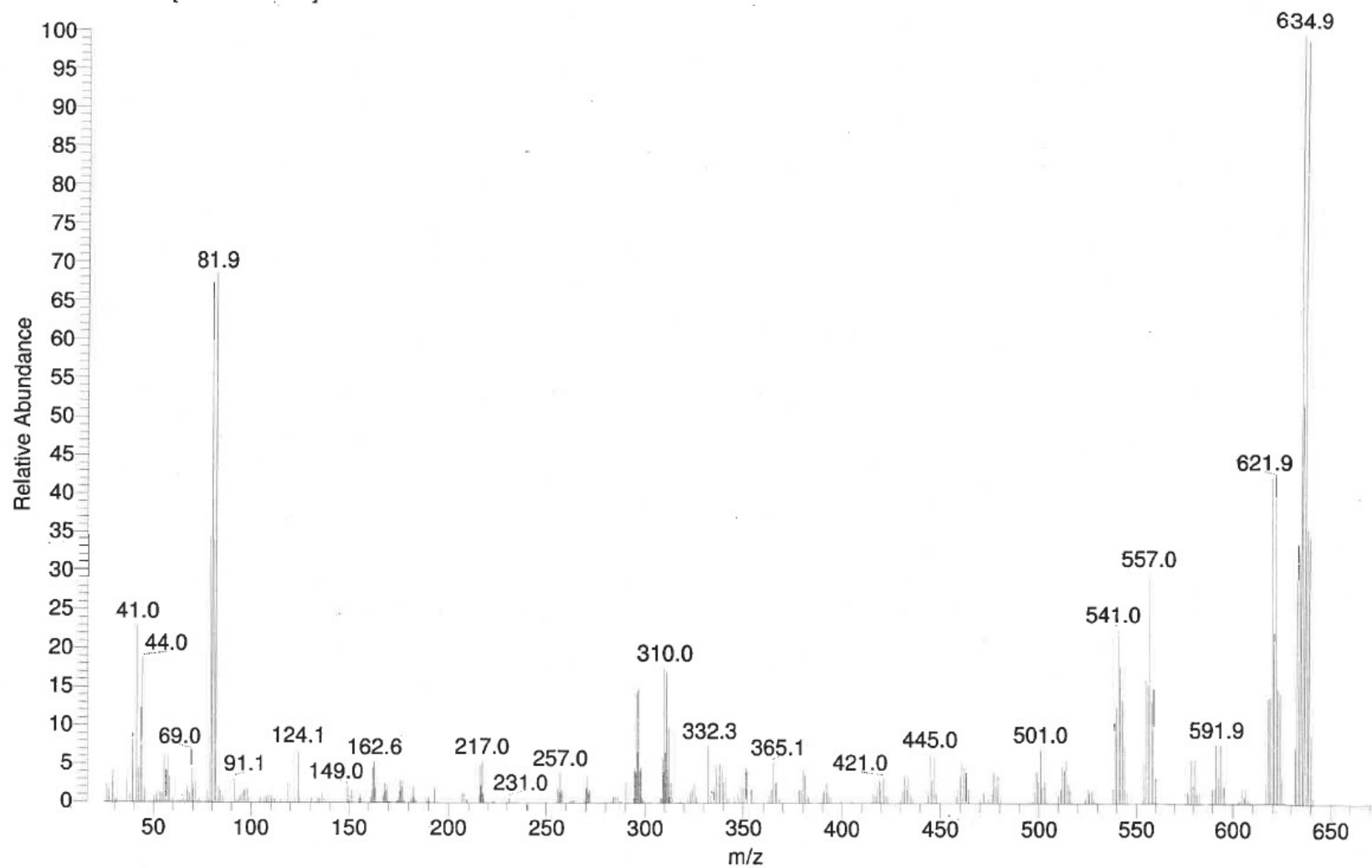


Figure S13: Low resolution mass spectrum of 6.

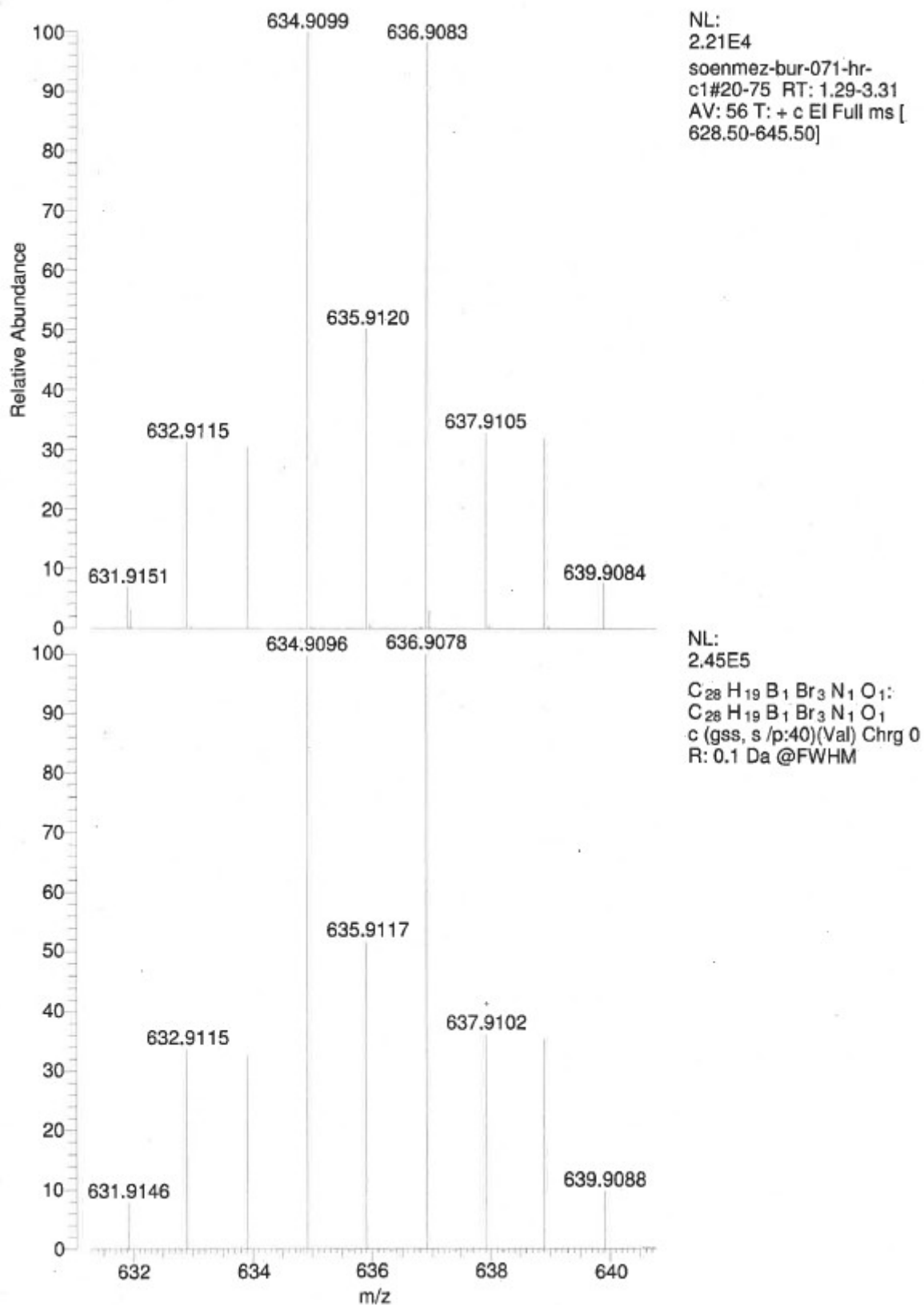


Figure S14: High resolution mass spectrum of 6.

Sünmez

Massenspektrometrie - Universität Stuttgart

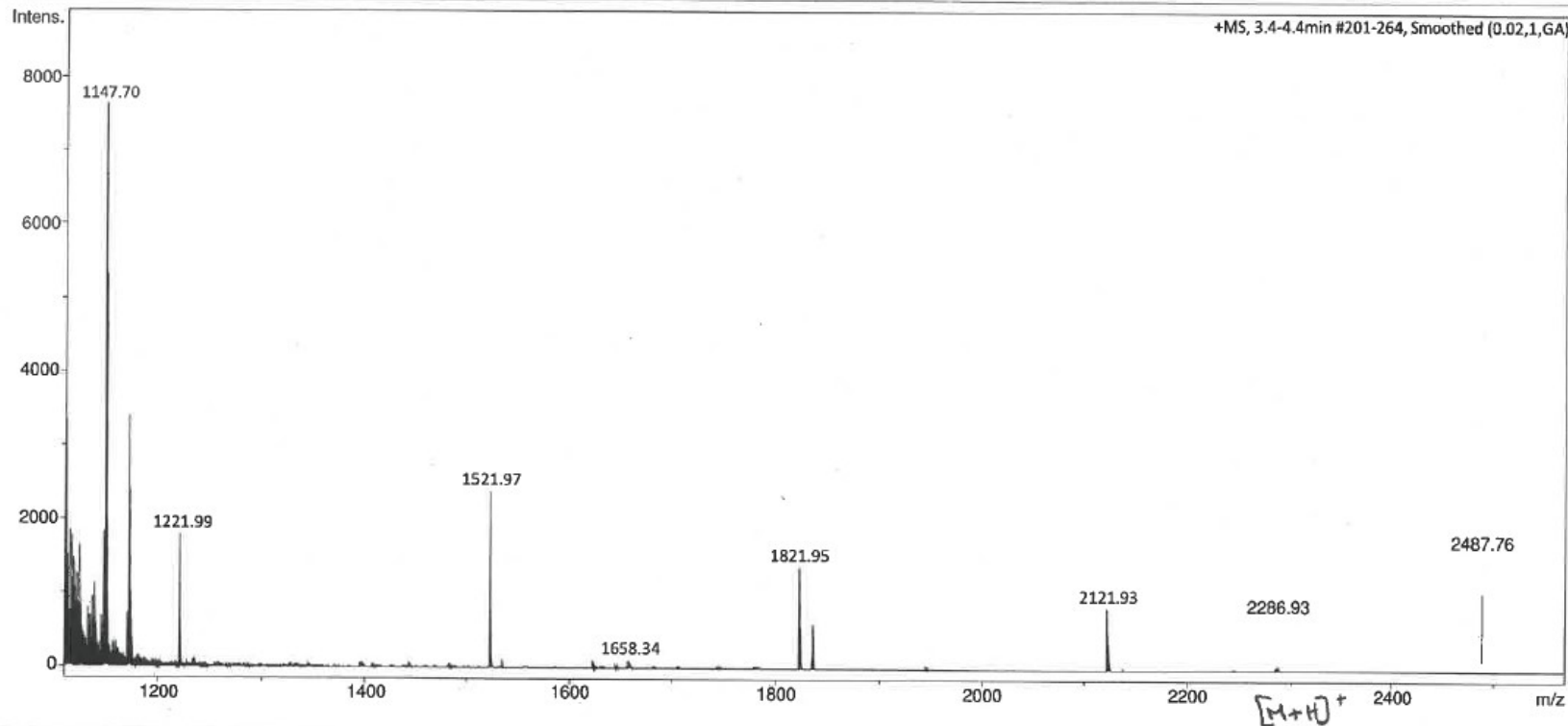
Analysis Info

Analysis Name Suenmez-BUR-072.d
Method tune-wide-oktober-2019.m
Sample Name Sünmez-BUR-072
Comment MeCN : CHCl₃ = 1:1

Acquisition Date 8/13/2021 3:25:04 PM
Operator BDAL@DE
Instrument micrOTOF-Q 228888.00043

Acquisition Parameter

Source Type	APCI	Ion Polarity	Positive	Set Nebulizer	1.7 Bar
Focus	Not active	Set Capillary	4500 V	Set Dry Heater	300 °C
Scan Begin	250 m/z	Set End Plate Offset	-500 V	Set Dry Gas	5.0 l/min
Scan End	3000 m/z	Set Collision Cell RF	500.0 Vpp	Set Divert Valve	Waste



Bruker Compass DataAnalysis 4.2

printed: 8/13/2021 3:39:37 PM

Page 1 of 1

Figure S15: Low resolution mass spectrum of BON-LC.

Massenspektrometrie - Universität Stuttgart

Analysis Info

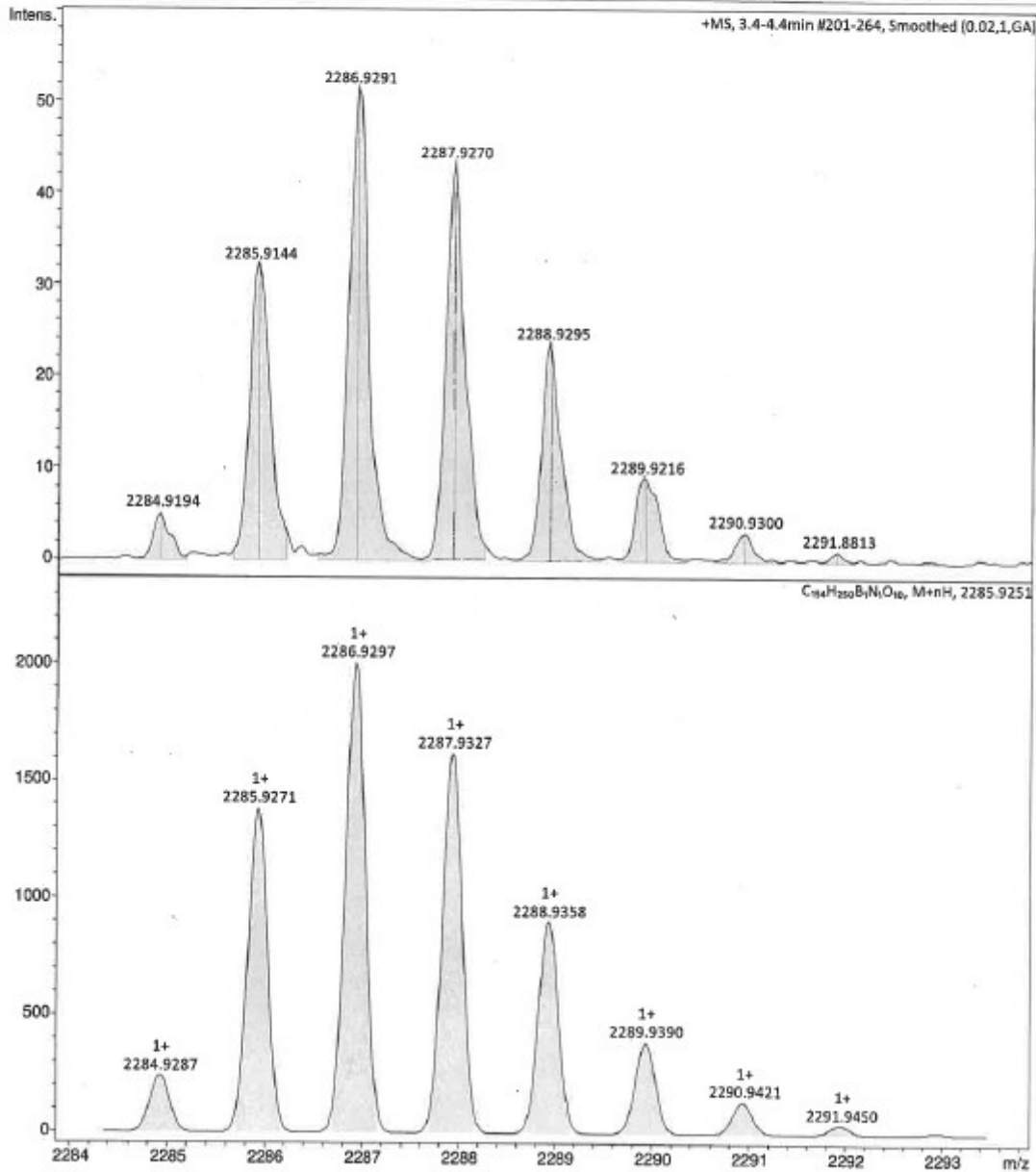
Analysis Name Suenmez-BUR-072.d
Method tune-wide-oktober-2019.m
Sample Name Sünmez-BUR-072
Comment MeCN : CHCl₃ = 1:1

Acquisition Date 8/13/2021 3:25:04 PM

Operator BDAL@DE
Instrument micrOTOF-Q 228888.00
043

Acquisition Parameter

Source Type	APCI	Ion Polarity	Positive	Set Nebulizer	1.7 Bar
Focus	Not active	Set Capillary	4500 V	Set Dry Heater	300 °C
Scan Begin	250 m/z	Set End Plate Offset	-500 V	Set Dry Gas	5.0 l/min
Scan End	3000 m/z	Set Collision Cell RF	500.0 Vpp	Set Divert Valve	Waste



Bruker Compass DataAnalysis 4.2

printed: 8/13/2021 3:37:59 PM

Page 1 of 1

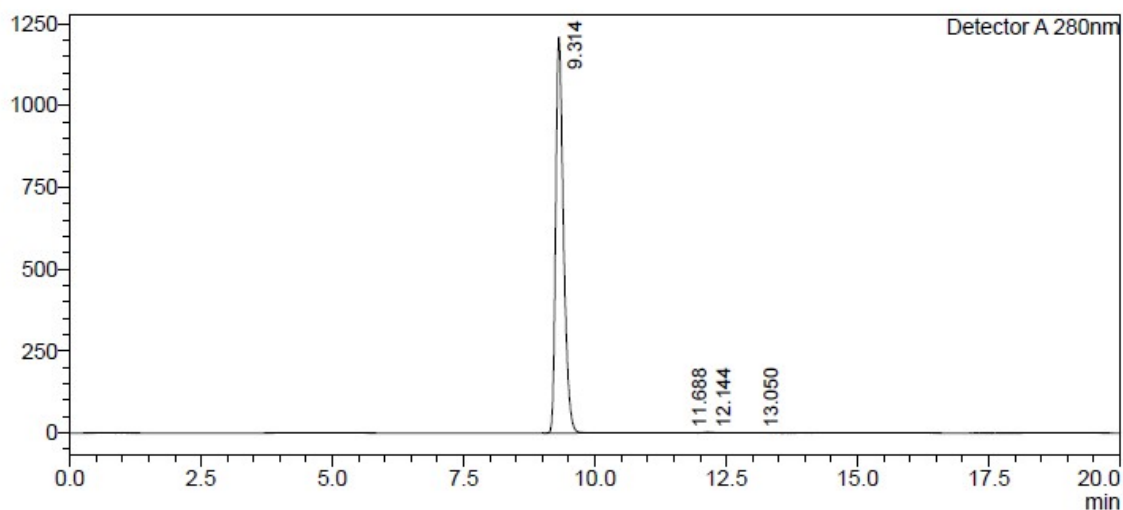
Figure S16: High resolution mass spectrum of BON-LC.

<Sample Information>

Sample Name : JK_4629_Fkt5
Sample ID : JK_4629_Fkt5
Method Filename : 100% THF 20 mins 280nm - new-please use.lcm
Batch Filename : JK_4629_prep.lcb
Vial # : 1-40
Injection Volume : 5 uL
Date Acquired : 21/06/2022 16:12:01
Date Processed : 21/06/2022 16:32:03
Sample Type : Unknown
Acquired by : System Administrator
Processed by : System Administrator

<Chromatogram>

mV



<Peak Table>

Detector A 280nm

Peak#	Ret. Time	Area	Height	Area%	Area/Height	Width at 5% Height
1	9.314	12507301	1208045	99.746	10.353	0.359
2	11.688	1680	116	0.013	14.520	0.330
3	12.144	27490	2654	0.219	10.356	0.350
4	13.050	2707	249	0.022	10.849	0.316
Total		12539178	1211064	100.000		

Figure S17: Analytical GPC report of BON-LC.

5. Electrochemical Properties of the BON-LC

Table S2: HOMO and LUMO energies of the **BON-LC** extracted from DPV measurements and HOMO/LUMO literature values of a similar B,O,N-PAH **B-O-Cz** for comparison.

Compound	$E_{\text{ox}}^{[a]}$ / eV	E_{HOMO} / eV	$E_{\text{red}}^{[a]}$ / eV	E_{LUMO} / eV
BON-LC	1.13	-5.93 ^[b]	-1.71	-3.09 ^[b]
B-O-Cz ^[25]	-	-6.03	-	-3.23

[a] referenced vs. standard calomel electrode in a N₂ saturated, 0.1 M solution of [ⁿBu₄N]PF₆ in CH₂Cl₂ via Ferrocene/Ferrocenium (Fc/Fc⁺) as internal standard (0.46 V vs SCE^[20]) $E_{\text{ox/red}} = E_{\text{peak}} + (0.46 \text{ V} - E_{1/2}(\text{Fc}/\text{Fc}^+))$. [b] The HOMO and LUMO values were extracted from the anodic / cathodic DPV peak potentials according to $E_{\text{HOMO/LUMO}} = -(E_{\text{ox}} / E_{\text{red}} + 4.8) \text{ eV}$.^[21]

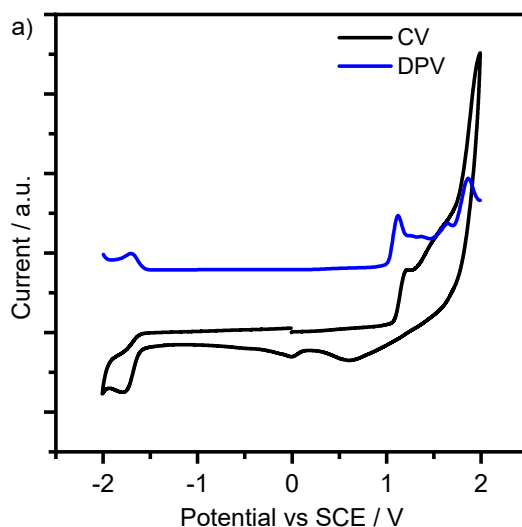


Figure S18: CV (black trace) and DPV (blue trace) of **BON-LC** recorded in a N₂ saturated, 0.1 M solution of [ⁿBu₄N]PF₆ in CH₂Cl₂ vs. Ferrocene/Ferrocenium as internal standard (0.46 V vs SCE,^[20] scan rate: 100 mV s⁻¹), SCE = standard calomel electrode.^[20]

6. Mesomorphic Properties

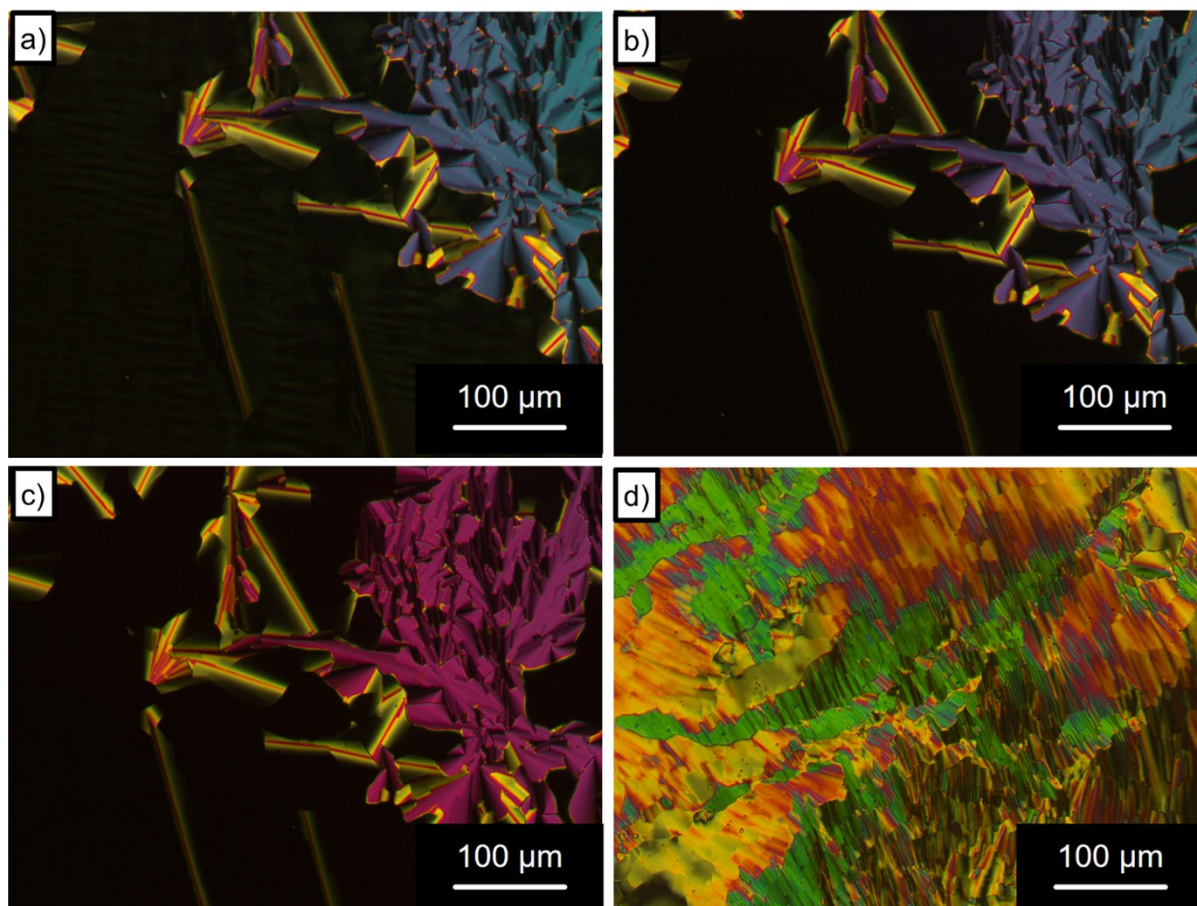


Figure S19: Textures obtained on the POM (crossed polarizers, sample sandwiched between two glass slides) upon cooling of **BON-LC** from the isotropic melt: a) at 10 °C, cooling rate: 10 K min⁻¹; b) 60 °C, cooling rate: 10 K min⁻¹; c) 120 °C, cooling rate: 10 K min⁻¹; d) 140 °C, 1 K min⁻¹, after shearing. The black areas correspond to homeotropic alignment of the sample.

Table S3: Phase transition temperature $T / ^\circ\text{C}$ and corresponding enthalpies $\Delta H / \text{kJ mol}^{-1}$ of **BON-LC** series during second heating (2nd H) and cooling (2nd C) cycles in the DSC measurements (heating/cooling rates: 10 K min⁻¹).

	Phase	$T / ^\circ\text{C}$ ($\Delta H / \text{kJ mol}^{-1}$)	Phase	$T / ^\circ\text{C}$ ($\Delta H / \text{kJ mol}^{-1}$)	Phase
2 nd H	G	22 (-) [a]	Col _{ho}	144.1 (7.2)	I
2 nd C	G	17 (-) [a]	Col _{ho}	144.8 (-7.2)	I

[a]: Glass transition temperature determined as midpoint ISO from DSC experiments.

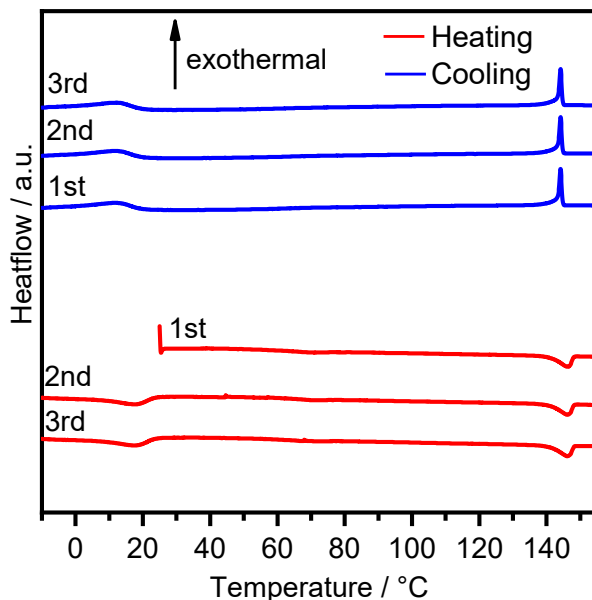


Figure S20: DSC thermograms (heating/ cooling rate: 10 K min⁻¹) of **BON-LC**.

Table S4: XRD data of **BON-LC**.

Mesophase	Lattice parameters	q / nm^{-1}	$d / \text{\AA}^{[a]}$	Miller indices
Col _{ho} at 33°C <i>p6mm</i>	$a = 35.92 \text{ \AA}$ $Z = 1$ $\rho = 0.78$	2.02	31.10	(10)
		3.49	18.00 (17.96)	(11)
		4.03	15.59 (15.55)	(20)
		5.35	11.74 (11.76)	(21)
		- [b]	- [b] (10.37)	(30)
		6.97	9.01 (8.98)	(22)
		7.27	8.64 (8.63)	(31)
		8.06	7.80 (7.78)	(40)
		14.17 [c]	4.43 [c]	(halo)
		18.00 [c]	3.49 [c]	(π - π)

[a]: Calculated d values are given in parentheses, [b] reflection not observed, [c] values obtained from two component Lorentzian fit of the wide angle regime.

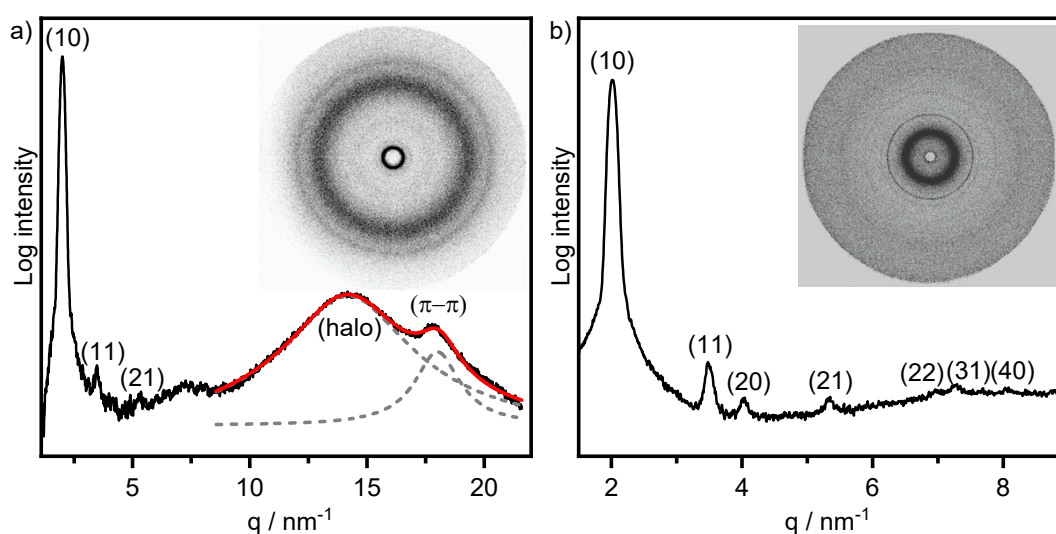


Figure S21: a) WAXS diffractogram of **BON-LC** recorded at 33 °C with the 2D WAXS pattern shown as inset. The red trace represents the fit of the wide-angle region with two Lorentzian functions (grey dashed traces); b) SAXS diffractogram recorded at 33 °C with the 2D SAXS pattern shown as inset.

7. Photophysical Properties

Table S5: Photophysical data of the **BON-LC** in dilute toluene solution, in a polystyrene film (PS film) and in a neat film.

solvent	$\lambda_{\text{abs}} / \text{nm}$	$\lambda_{\text{PL}} / \text{nm}$	FWHM / nm (FWHM / eV)	Stokes shift / cm^{-1} (stokes shift / eV)	$\Phi / \text{a.u.}$	$\tau_{\text{p}} / \text{ns}$	$\Delta E_{\text{ST}} / \text{eV}$
toluene (0.02 mM)	448	466	23 (130)	862.2 (106.9)	0.77	6.75	0.25
PS (1 wt%)	454	467	45 (249)	613.2 (76.0)	0.90	9.85	n.d.
neat	455	544	77 (327)	3595.7 (445.8)	0.39	31.96	n.d.

Table S6: Solvatochromism and Solvatofluorochromism data of the **BON-LC** series in solvents of different polarity.

methylcyclohexane	Toluene		THF		CH_2Cl_2		Butyronitrile		
$E_{\text{T}}(30) / \text{kcal} \cdot \text{mol}^{-1}$	$\sim 31^{[a]}$		33.9 ^[26]		37.4 ^[26]		40.7 ^[26]		42.5 ^[26]
$\lambda_{\text{abs}} / \text{nm}$	$\lambda_{\text{PL}} / \text{nm}$	$\lambda_{\text{abs}} / \text{nm}$	$\lambda_{\text{PL}} / \text{nm}$	$\lambda_{\text{abs}} / \text{nm}$	$\lambda_{\text{PL}} / \text{nm}$	$\lambda_{\text{abs}} / \text{nm}$	$\lambda_{\text{PL}} / \text{nm}$	$\lambda_{\text{abs}} / \text{nm}$	$\lambda_{\text{PL}} / \text{nm}$
446	459	448	466	449	467	449	470	449	471

[a]: no $E_{\text{T}}(30)$ value reported for methylcyclohexane. Other aliphatics have an $E_{\text{T}}(30) \sim 31 \text{ kcal} \cdot \text{mol}^{-1}$ and this value is given as rough estimate for methylcyclohexane. ^[26]

Table S7: Fitting parameters of the triple/ double exponential fits of the TCSPC measurements of the **BON-LC** in a polystyrene film (PS film) and in a neat film.

solvent	τ_1 / ns	$A_1 / \text{a.u.}$	τ_2 / ns	$A_2 / \text{a.u.}$	τ_3 / ns	$A_3 / \text{a.u.}$	$\tau_{\text{avg}} / \text{ns}$	$\chi^2 / \text{a.u.}$
toluene (0.02 mM)	6.75	24842.44	-	-	-	-	-	1.14
PS (1 wt%)	5.59	86238.35	12.59	48965.41	64.52	4255.82	9.85	1.26
neat	25.92	14940.01	47.58	5781.71	-	-	31.96	1.03

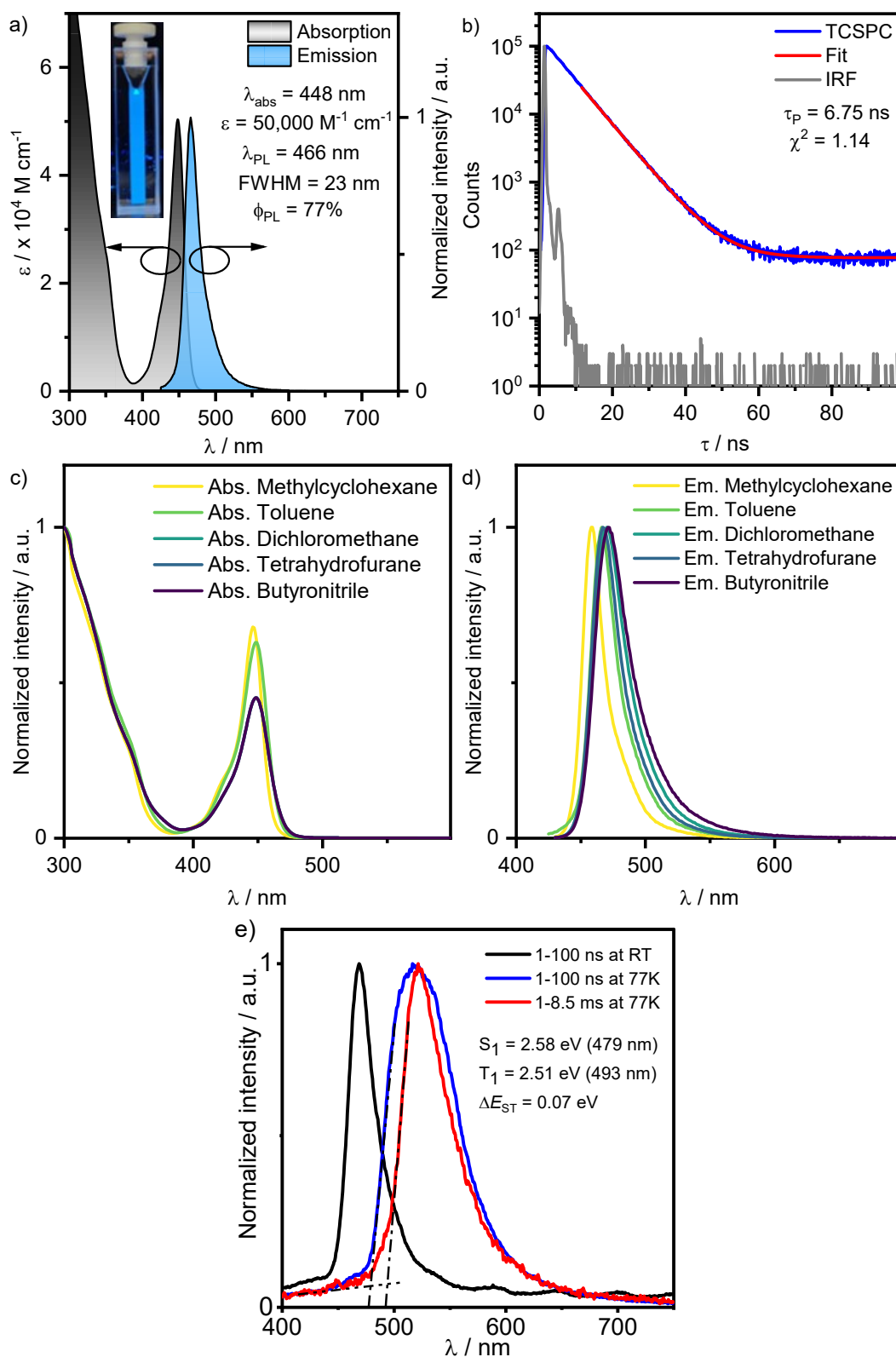


Figure S22: Solution photophysics of **BON-LC** in degassed toluene ($c = 0.02$ mM): a) steady-state absorption (black trace) and emission (blue trace) ($\lambda_{\text{exc}} = 350$ nm); b) luminescence decay (blue trace) with monoexponential fit (red trace) and IRF (grey trace) in the ns range ($\lambda_{\text{exc}} = 375$ nm); c) solvatochromism in different solvents ($c = 0.02$ mM); d) solvatofluorochromism in different solvents ($c = 0.02$ mM, $\lambda_{\text{exc}} = 350$ nm); e) fluorescence (red trace), phosphorescence (blue trace) and corresponding onsets as S_1 and T_1 energies at 77K in a frozen toluene matrix ($\lambda_{\text{exc}} = 350$ nm).

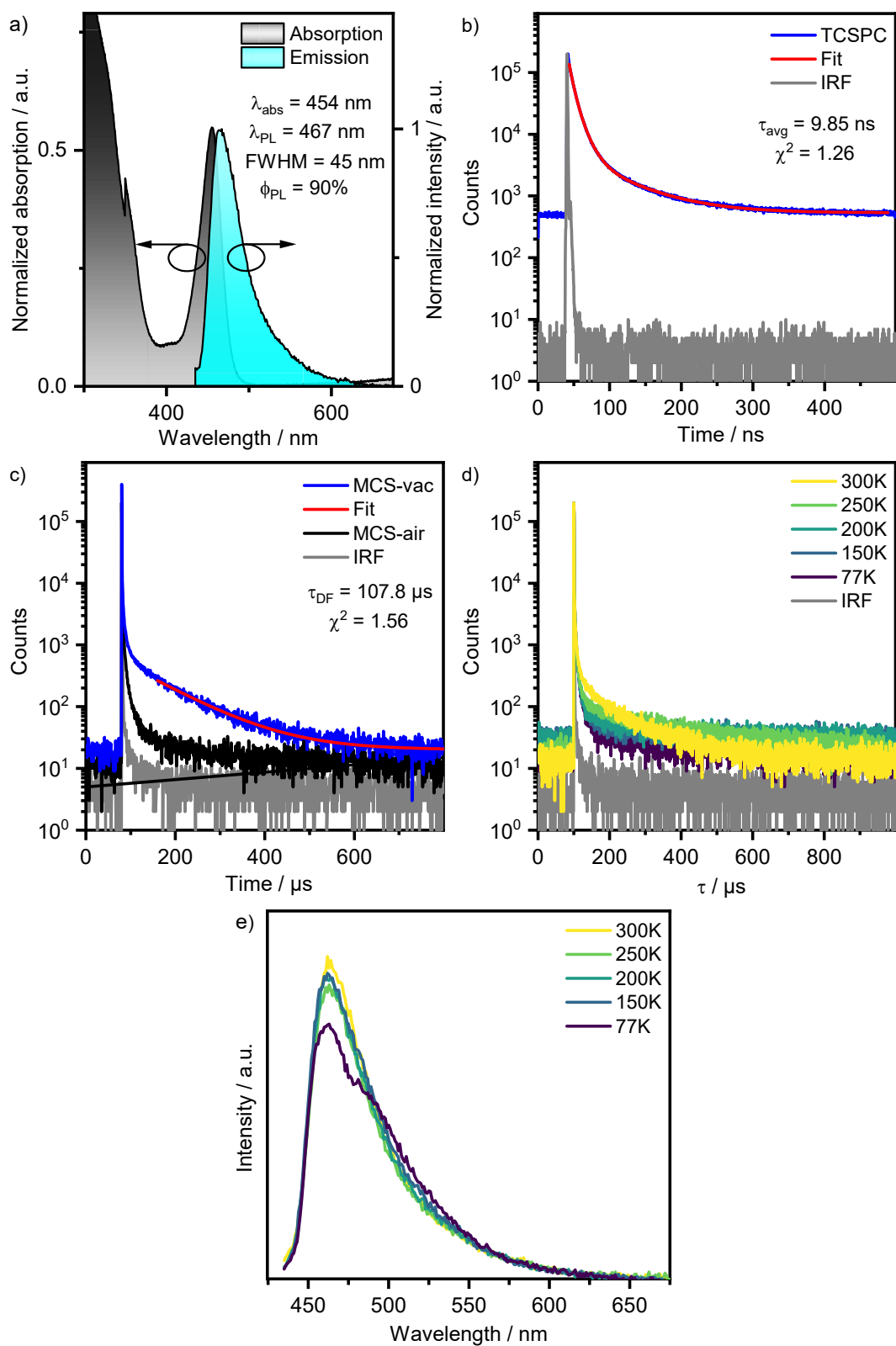


Figure S23: Photophysics of **BON-LC** in a polystyrene (PS) film ($c = 1$ wt%): a) absorption (black trace) and steady-state emission (blue trace, $\lambda_{\text{exc}} = 350$ nm), inset shows the film under UV light; b) luminescence decay (blue trace) with triexponential fit (red trace) and IRF (grey trace) in the ns range ($\lambda_{\text{exc}} = 379$ nm); c) luminescence decay under air (black trace) and vacuum (blue trace) and IRF (grey trace) in the μs range ($\lambda_{\text{exc}} = 379$ nm); d) temperature dependent luminescence decay in the μs range ($\lambda_{\text{exc}} = 379$ nm); e) temperature dependent steady-state photoluminescence ($\lambda_{\text{exc}} = 350$ nm).

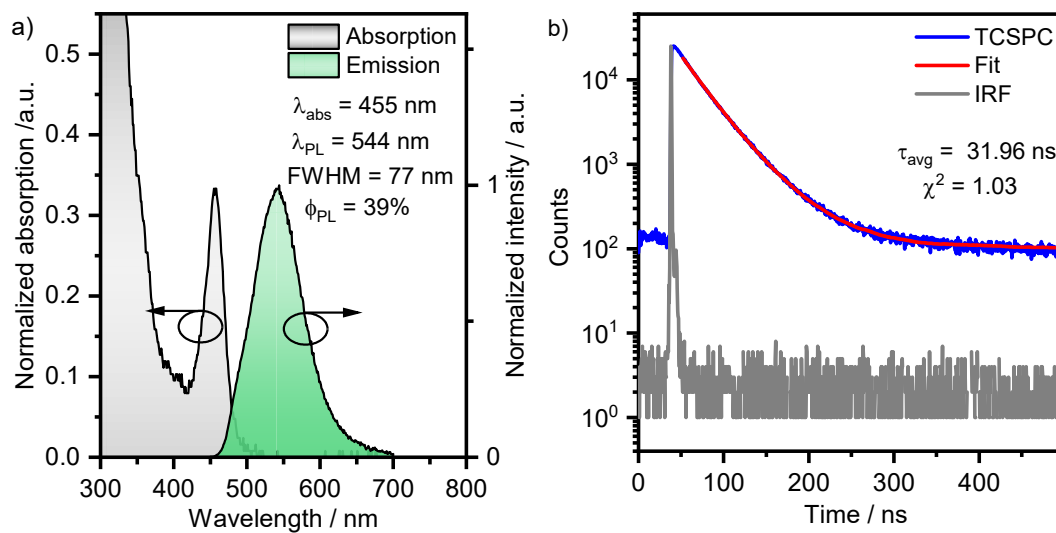


Figure S24: Photophysics of **BON-LC** in a spin coated film: a) steady-state absorption (black trace) and emission (green trace) ($\lambda_{\text{exc}} = 350 \text{ nm}$), inset shows the film under UV light; b) luminescence decay (blue trace) with biexponential fit (red trace) and IRF (grey trace) in the ns range ($\lambda_{\text{exc}} = 379 \text{ nm}$).

8. Literature

- [1] D. B. G. Williams, M. Lawton, *J. Org. Chem.* **2010**, *75*, 8351–8354.
- [2] S. Hitosugi, D. Tanimoto, W. Nakanishi, H. Isobe, *Chem. Lett.* **2012**, *41*, 972–973.
- [3] G. R. Fulmer, A. J. M. Miller, N. H. Sherden, H. E. Gottlieb, A. Nudelman, B. M. Stoltz, J. E. Bercaw, K. I. Goldberg, *Organometallics* **2010**, *29*, 2176–2179.
- [4] Gaussian 16, Revision C.01, M. J. Frisch, G. W. Trucks, H. B. Schlegel, G. E. Scuseria, M. A. Robb, J. R. Cheeseman, G. Scalmani, V. Barone, G. A. Petersson, H. Nakatsuji, X. Li, M. Caricato, A. V. Marenich, J. Bloino, B. G. Janesko, R. Gomperts, B. Mennucci, H. P. Hratchian, J. V. Ortiz, A. F. Izmaylov, J. L. Sonnenberg, D. Williams-Young, F. Ding, F. Lipparini, F. Egidi, J. Goings, B. Peng, A. Petrone, T. Henderson, D. Ranasinghe, V. G. Zakrzewski, J. Gao, N. Rega, G. Zheng, W. Liang, M. Hada, M. Ehara, K. Toyota, R. Fukuda, J. Hasegawa, M. Ishida, T. Nakajima, Y. Honda, O. Kitao, H. Nakai, T. Vreven, K. Throssell, J. A. Montgomery, Jr., J. E. Peralta, F. Ogliaro, M. J. Bearpark, J. J. Heyd, E. N. Brothers, K. N. Kudin, V. N. Staroverov, T. A. Keith, R. Kobayashi, J. Normand, K. Raghavachari, A. P. Rendell, J. C. Burant, S. S. Iyengar, J. Tomasi, M. Cossi, J. M. Millam, M. Klene, C. Adamo, R. Cammi, J. W. Ochterski, R. L. Martin, K. Morokuma, O. Farkas, J. B. Foresman, and D. J. Fox, Gaussian, Inc., Wallingford CT, **2016**.
- [5] F. Neese, *WIREs Comput. Mol. Sci.* **2012**, *2*, 73–78.
- [6] F. Neese, *WIREs Comput. Mol. Sci.* **2022**, *12*, e1606.
- [7] C. Adamo, V. Barone, *J. Chem. Phys.* **1999**, *110*, 6158–6170.
- [8] G. A. Petersson, T. G. Tensfeldt, J. A. Montgomery, *J. Chem. Phys.* **1991**, *94*, 6091–6101.
- [9] M. Casanova-Páez, L. Goerigk, *J. Chem. Theory Comput.* **2021**, *17*, 5165–5186.
- [10] R. A. Kendall, T. H. Dunning, R. J. Harrison, *J. Chem. Phys.* **1992**, *96*, 6796–6806.
- [11] O. S. Lee and E. Zysman-Colman, Silico (version 5.0), In-Silico-Computing, St Andrews, Scotland, **2023**.
- [12] N. M. O’boyle, A. L. Tenderholt, K. M. Langner, *J. Comput. Chem.* **2008**, *29*, 839–845.
- [13] W. Humphrey, A. Dalke, K. Schulten, *J. Mol. Graphics* **1996**, *14*, 33–38.
- [14] J. E. Stone, An efficient library for parallel ray tracing and animation, **1998**.
- [15] N. M. O’Boyle, M. Banck, C. A. James, C. Morley, T. Vandermeersch, G. R. Hutchison, *J. Cheminf.* **2011**, *3*, 33.
- [16] N. M. O’Boyle, G. R. Hutchison, *Chem. Cent. J.* **2008**, *2*, 24.
- [17] A. Sillen, Y. Engelborghs, *Photochem. Photobiol.* **1998**, *67*, 475–486.
- [18] G. A. Crosby, J. N. Demas, *J. Phys. Chem.* **1971**, *75*, 991–1024.
- [19] A. M. Brouwer, *Pure Appl. Chem.* **2011**, *83*, 2213–2228.
- [20] N. G. Connelly, W. E. Geiger, *Chem. Rev.* **1996**, *96*, 877–910.
- [21] C. M. Cardona, W. Li, A. E. Kaifer, D. Stockdale, G. C. Bazan, *Adv. Mater.* **2011**, *23*, 2367–2371.
- [22] F. Leroux, T. U. Hutschenreuter, C. Charrière, R. Scopelliti, R. W. Hartmann, *Helv. Chim. Acta* **2003**, *86*, 2671–2686.
- [23] T. Yasuda, T. Shimizu, F. Liu, G. Ungar, T. Kato, *J. Am. Chem. Soc.* **2011**, *133*, 13437–13444.
- [24] H. Maeda, Y. Haketa, T. Nakanishi, *J. Am. Chem. Soc.* **2007**, *129*, 13661–13674.
- [25] J. Park, J. Lim, J. H. Lee, B. Jang, J. H. Han, S. S. Yoon, J. Y. Lee, *ACS Appl. Mater. Interfaces* **2021**, *13*, 45798–45805.
- [26] C. Reichardt, T. Welton, in *Solvents and Solvent Effects in Organic Chemistry*, Wiley, **2010**, 425 - 508.